Environment International 178 (2023) 108037

Contents lists available at ScienceDirect

Environment International

journal homepage: www.elsevier.com/locate/envint

Full length article

Historical trends of traditional, emerging, and halogenated polycyclic aromatic hydrocarbons recorded in core sediments from the coastal areas of the Yellow and Bohai seas

Seo Joon Yoon [a], Seongjin Hong [b,*], Junghyun Lee [a], Jongmin Lee [a], Youngnam Kim [b], Moo Joon Lee [c], Jongseong Ryu [c], Kyungsik Choi [a], Bong-Oh Kwon [d], Wenyou Hu [e], Tieyu Wang [f], Jong Seong Khim [a,*]

[a] School of Earth and Environmental Sciences & Research Institute of Oceanography, Seoul National University, Seoul 08826, Republic of Korea
[b] Department of Marine Environmental Science, Chungnam National University, Daejeon 34134, Republic of Korea
[c] Department of Marine Biotechnology, Anyang University, Incheon, Ganghwagun 23038, Republic of Korea
[d] Department of Marine Biotechnology, Kunsan National University, Kunsan 54150, Republic of Korea
[e] Key Laboratory of Soil Environment and Pollution Remediation, Institute of Soil Science, Chinese Academy of Sciences, Nanjing 210008, China
[f] Institute of Marine Sciences, Shantou University, Shantou 515063, China

ARTICLE INFO

Keywords:
Emerging pollutants
Deposition flux
Mass inventory
Coastal area
East Asia

ABSTRACT

Historical trends of polycyclic aromatic hydrocarbons (PAHs) contamination were reconstructed from eleven sediment cores located in intertidal zones of the Yellow and Bohai seas for a period encompassing the last 80 years. The analysis encompassed 15 traditional PAHs (t-PAHs), 9 emerging PAHs (e-PAHs), and 30 halogenated PAHs (Hl-PAHs), including 10 chlorinated PAHs (Cl-PAHs) and 20 brominated PAHs (Br-PAHs). Concentrations of target PAHs were highest in industrial and municipal areas situated along the coast of the Bohai Sea, including Huludao, Yingkou, Tianjin, and Dandong, constituting a substantial mass inventory. All target PAHs showed increasing trends since the 1950s, reflecting the development history of South Korea and China. High molecular weight PAHs accumulated in sampling sites more than low molecular weight PAHs. A positive matrix factorization model showed that the PAH sources were coal and gasoline combustion (35%), diesel combustion (33%), and biomass combustion (32%). Over the last 80 years, the contribution of coal and gasoline combustion increased in all regions, while diesel combustion and biomass combustion varied across regions and over time. Toxicity equivalence values were highest for t-PAHs (>99% contribution), followed by Cl-PAHs, Br-PAHs, and e-PAHs. Concentrations of t-PAHs in Eastern Asia seas have increased since the 1900s, particularly in intertidal areas compared to subtidal areas. The intertidal zone removed 83% of the total flux of PAHs originating from land and thus appears to serve as a buffer zone against marine pollution. Overall, this study provides novel knowledge on the historical trends and sources of PAHs on a large scale, along with insights for future coastal management.

1. Introduction

Reconstructing the contamination trends in persistent toxic substances (PTSs) from sediment cores can provide valuable insights into environmental changes that occur during economic development and energy consumption (Liu et al., 2012; Zhang et al., 2013; Chen et al., 2016). Determining the deposition flux and inventory of PTSs can provide knowledge about contamination trends and stocks on both regional and large marine ecosystem (LME) scales, which can support environmental management in contaminated areas (Liu et al., 2011; Wang et al., 2017). Previous studies have focused primarily on elucidating contamination trends on regional scales, including the subtidal zones of estuaries, bays, coasts, and offshore areas (Liu et al., 2005; Guo et al., 2006; Yan et al., 2009; Zhang et al., 2009; Hu et al., 2011; Li et al., 2015; Cai et al., 2016; Guerra et al., 2019). However, limited information is available on the contamination history of classical PTSs, including traditional polycyclic aromatic hydrocarbons (t-PAHs) and organochlorine chemicals, from the intertidal area with only a few sites

* Corresponding authors.
E-mail addresses: hongseongjin@cnu.ac.kr (S. Hong), jskocean@snu.ac.kr (J.S. Khim).

https://doi.org/10.1016/j.envint.2023.108037
Received 1 February 2023; Received in revised form 18 May 2023; Accepted 12 June 2023
Available online 15 June 2023

(Zhang et al., 2013; Kaiser et al., 2016). In addition, although deposition fluxes have also been reported for a wide range of eastern China marginal seas, only t-PAHs from surface sediments were analyzed in the absence of historical information (Wang et al., 2017). Thus, there remains a need to assess the contamination history of emerging PTSs in intertidal areas.

Emerging-PAHs (e-PAHs) are substituted amino-, cyano-, and alkyl-PAHs that have physicochemical properties similar to those of t-PAHs. These compounds originate from coal tar, coal, wood, and traffic sources (Benner et al., 1995; Li and Ellis, 2015; Kucharova et al., 2013). e-PAHs have high toxic potential, including mutagenicity, genotoxicity, and developmental toxicity (Gibson et al., 1978; LaVoie et al., 1983; Onodera et al., 1994; Mimura and Fujii-Kuriyama, 2003; Cha et al., 2019; Kim et al., 2019a). Previous studies have explored the occurrences and distribution of e-PAHs from estuaries, bays, coasts, and offshore areas (An et al., 2020; Cha et al., 2019; Gwak et al., 2022, Hong et al., 2022; Kim et al., 2019a, Kim et al., 2021). However, the vertical distribution and deposition flux of e-PAHs has yet to be elucidated.

Halogenated-PAHs (Hl-PAHs), including chlorinated-PAHs (Cl-PAHs) and brominated PAHs (Br-PAHs), originate from incomplete combustion with specific halogen sources, such as may occur in waste incineration (Fujima et al., 2006; Miyake et al., 2017). Hl-PAH compounds are carcinogenic and mutagenic (Fu et al., 1996, 1999; Ohura et al., 2010). Several Hl-PAHs are more toxic than the toxicity standard reference molecule benzo[*a*]pyrene (BaP), including 7-monobromobenz[*a*]anthracene, 7-chlorobenzo[*a*]anthracene, 3,8-dichlorofluoranthene, 4,7-dibromobenz[*a*]anthracene, and 6-chlorochrysene (Ohura et al., 2007; Horii et al., 2009a). Distributions of Hl-PAHs have been examined primarily in gases and particle samples in the air, waste incineration products, and discharge from wastewater treatment plants in freshwater environments (Horii et al., 2008; Li et al., 2019a; Myers et al., 2014; Ohura et al., 2009, 2018, Sun et al., 2011, 2012, Vuong et al., 2020a,b). However, few studies have been conducted in coastal and offshore areas (Horii et al., 2009b; Ohura et al., 2015; Sei et al., 2021). Hl-PAH distribution data have been reported for some marine environment regions, but the major specific sources of Hl-PAHs in coastal areas have yet to be elucidated (Ohura et al., 2015). Furthermore, knowledge regarding the distribution and deposition flux of Hl-PAHs in the intertidal zone remains limited.

Identifying and quantifying contaminant sources are important processes for enabling contamination changes to be tracked and controlled. Positive matrix factorization (PMF) is a multivariate analysis modeling technique whose features complement the weaknesses of qualitative evaluation; notably, PMF has the advantages of not requiring source profiles and having the ability to handle extensive monitoring datasets (Paatero and Tapper, 1994). PMF models have been used

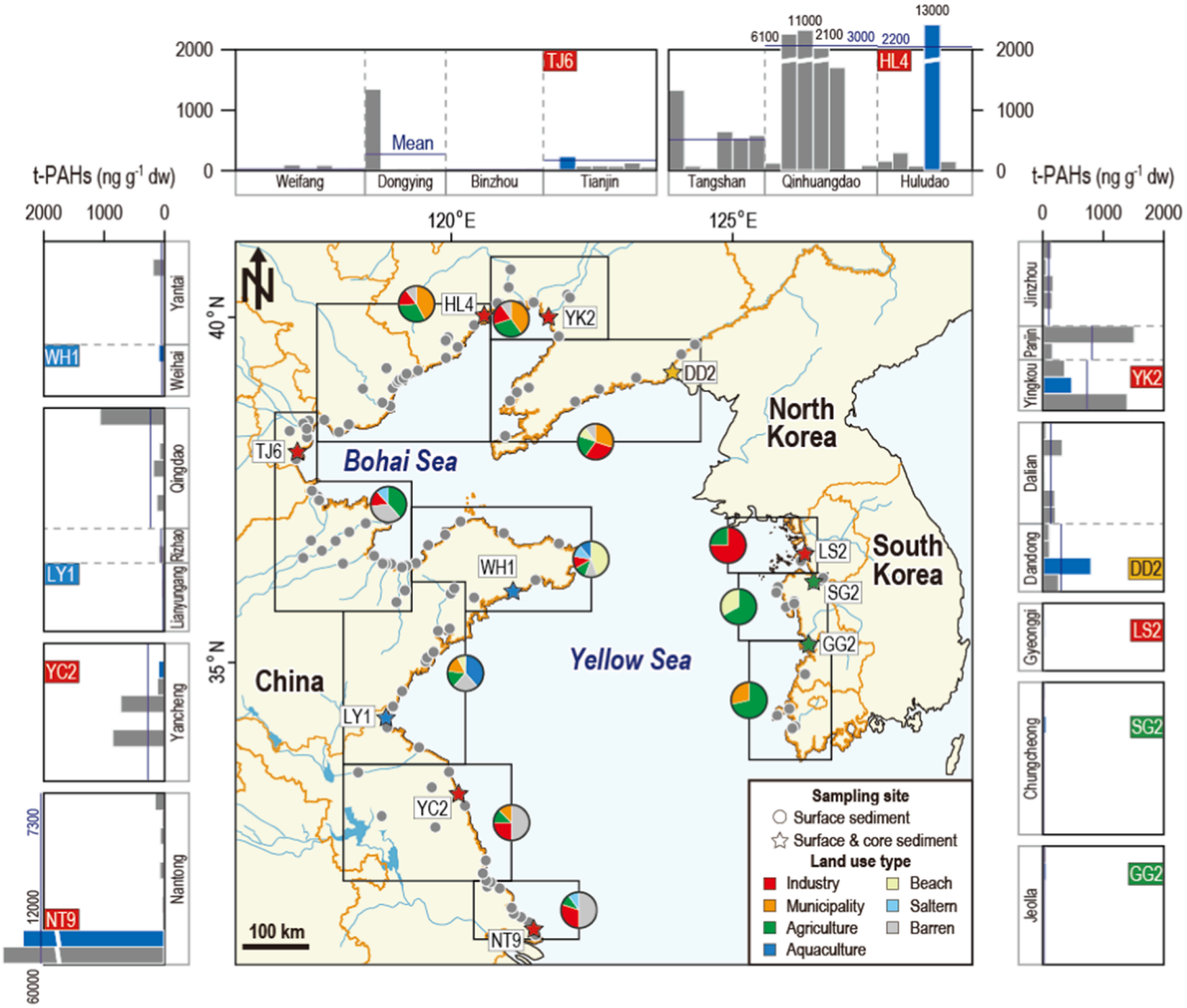

Fig. 1. Map showing the study area, sampling sites, and concentration of t-PAHs in surface sediment in a previous study (Yoon et al., 2020) for the Yellow and Bohai seas. Sediment cores were collected from sites marked with stars, and land use types were based on the previous study.

previously to identify contaminant sources from various environmental matrices, including biomass, coal tar, coke oven, diesel, gasoline, natural gas, oil burning, surface pavement, and vehicular emissions (Jeddi et al., 2022; Li et al., 2019b; Zeng et al., 2018; Zhang et al., 2019).

The Yellow Sea Large Marine Ecosystem (YSLME), which is semi-closed and borders the Korean peninsula and northeast China, is highly developed (Hoagland and Jin, 2006). Rapid developments in the YSLME region have caused PTSs discharge which is producing intensive pressure on YSLME. Severe contamination with many environmental pollutants, including both classic and emerging PTSs, has been reported for three decades (Khim et al., 2018a). Our research group has been undertaking extensive documentation of the pollution status in YSLME since the late 2000s (Hong et al., 2012; Meng et al., 2017; Khim et al., 2018b; Kim et al., 2020; Tian et al., 2020; Yoon et al., 2020). Previous research has been conducted from rivers to coastal areas on an LME scale that encompasses multiple land-use types (Yoon et al., 2020). However, historical trends of emerging PTSs from core sediments remain to be evaluated on an LME scale and for the intertidal zone.

The aim of this study was to examine the historical contamination trends of t-PAHs, e-PAHs, Cl-PAHs, and Br-PAHs in YSLME tidal flats (Fig. 1). The main objectives included: (1) determining vertical deposition with mass inventory; (2) reconstructing historical contamination trends; (3) tracing changes to compositional profiles and sources; (4) evaluating potential toxicity from past to present; and (5) delineating contamination history, flux, and inventory in East Asia. To the best of our knowledge, the presently reported data represent the first historical trend information for e-PAHs, Cl-PAHs, and Br-PAHs in tidal flats on an LME scale.

2. Materials and methods

2.1. Study area

Core sediments were collected from the intertidal zone across seven provinces along the coast of South Korea and China in 2018 (Fig. 1). Eleven sampling sites were selected based on t-PAHs concentrations, sediment grain size, inter-site distance, and land use type, as determined in a previous study (Yoon et al., 2020). Sediment cores were collected with steel cores (100 mm high) and preserved in brown glass containers at –20 ℃.

2.2. Quantification of target PAHs

For PAH analysis, 15 t-PAHs, 9 e-PAHs, 30 Hl-PAHs (10 Cl- and 20 Br-PAHs), 4 surrogate standards (SS, acenaphthene-d_{10}, phenanthrene-d_{10}, chrysene-d_{12}, and perylene-d_{12}) and an internal standard (IS, 2-fluorobiphenyl) were purchased from AHH Chemical Co., Ltd. (Changzhou, China), ChemService (West Chester, PA, USA), Chiron (Trondheim, Norway), Santa Cruz Biotechnology, Inc. (Dallas, TX, USA), Sigma-Aldrich (Saint Louis, MO, USA), and Tokyo Chemical (Tokyo, Japan), respectively. Detailed information about the target compounds is presented in Table S1 of Supplementary Materials.

Two previously published methods of sediment treatment in preparation for PAHs analysis were employed with slight modifications (An et al., 2020; Vuong et al., 2020a). In brief, 5 g of freeze-dried sediments were extracted by Soxhlet extractor. Four SS were added to the sedmient sample before extraction. The extracts were concentrated, and activated copper powder (Sigma Aldrich) was added to the concentrate, which was then refined through a column containing activated silica gel (70–230 mesh, Sigma-Aldrich) and eluted with a 60 mL mixture of 20% dichloromethane and 80% hexane (Burdick & Jackson, Muskegon, MI). The eluents were concentrated with gentle nitrogen gas, and finally, IS was added. Target PAHs were determined by operating an Agilent 7890B gas chromatography coupled to a 5977B mass selective detector (Agilent Technologies, Santa Clara, CA, USA).

The instrument operating conditions for target PAH detection are presented in Table S2. The method detection limits (MDLs) for t-PAHs, e-PAHs, and Hl-PAHs were 0.07–0.89 ng g^{-1}, 0.12–0.81 ng g^{-1}, and 0.25–1.27 ng g^{-1}, respectively (Table S1). The recovery rates of acenaphthene-d_{10}, phenanthrene-d_{10}, chrysene-d_{12}, and perylene-d_{12} were generally acceptable at 78 ± 18%, 83 ± 9%, 94 ± 10%, and 86 ± 12%, respectively.

2.3. Sediment dating and calculations of deposition flux and inventory

The sediment accumulation rate (SAR) in YSLME was determined by dating sediment cores with a ^{210}Pb using a gamma-ray spectrometer coupled to a high-purity Germanium detector (Mirion Technologies, GA, USA), as described in detail by Cho et al. (2015). The constant flux constant sedimentation model was used due to the absence of ^{137}Cs, which is typically used to calibrate the constant rate of the supply model (Crozaz et al., 1964; Guo et al., 2020). Available values of excess ^{210}Pb activity ($^{210}Pb_{ex}$) values were detected in four YSLME study regions, namely YC2, TJ6, DD2, and SG2 (Fig. S1). Core section ages were estimated using Eq. (1),

$$lnC_i = lnC_0 - \frac{\lambda}{r}(m_i) \quad (1)$$

Where λ is a radioactive decay constant for excess ^{210}Pb (0.03114 yr^{-1}), and r is SAR. After obtaining the regression line equation, SAR was calculated as $-\lambda$ divided by the slope of the linear regression between $\ln^{210}$Pb and depth. Total organic carbon (TOC) was determined after decarbonization with an Elemental Analyzer (Elementar, Gmbh, Hanau, Germany). Bulk density was calculated from TOC values with a logarithmic equation as described previously (Avnimelech et al., 2001). PAH deposition flux (F) values were determined with Eq. (2),

$$F = C_x \times p_x \times S \quad (2)$$

Where S is the SAR for core sediment (cm y^{-1}), p_x is the bulk density at x depth in sediment (g cm^{-3}), and C_x is the concentration of the target PAHs at a depth of x (ng g^{-1}). Mass inventory (I) was determined using Eq. (3):

$$I = C_x \times Ai \times p_x \times d \quad (3)$$

Where Ai is the extent of the region (km^2), and d is the core sediment depth. Extent values for sampling area regions were obtained from a previous study (Yim et al., 2018). Sediment depth was set to be 0.5 m, matching the depth of the samples. The SARs in this study (range 0.27–1.28 cm yr^{-1}) correspond to a start date in 1952 and thus indicate an age of eight decades (Fig. S1).

2.4. Potential toxicity evaluation

The toxicity equivalence values (TEQ) were determined for all target PAHs based on their relative equivalency potencies (RePs) to BaP (Table S3). These RePs relate to AhR-mediated activities determined by YCM3 yeast cell bioassays in previous studies (Ohura et al., 2007; Ohura et al., 2009, 2018). Following the toxicity of 2,3,7,8-tetrachlorodibenzo-p-dioxin to target PAHs (Ohura et al., 2007), TEQ values were calculated using Eq. (4),

$$TEQ = \sum [C_i] \times ReP_{BaP,i}/60 \quad (4)$$

Where C_i is the concentration of compounds and $ReP_{BaP,i}$ represents ReP_{BaP} of compound i.

2.5. Data analyses

PMF modeling was conducted to identify sources for an EPA program in the USA employing a previously detailed method (Yoon et al., 2020). Overall, the model outcomes were considered acceptable (slope range 0.50–1.18; coefficient of determination range 0.79–1.00). However,

acenaphthene (Ace, 0.68), benzo[*b*]naphtho[2,3-*d*]furan (BBNF, 0.55), and 9,10-dichlorophenanthrene (9,10-Cl-Phe, 0.28) had low R^2 values. Statistical tests were performed in SPSS 25.0 and PRIMER 6. Cluster analysis was carried out with sites grouped spatially based on Euclidean distance. Spearman correlation was used to detect relationships among target PAHs, owing to non-parametric dispersion. Kruskal-Wallis testing was performed to detect differences between land-use types, and Mann-Whitney testing was carried out after the Bonferroni correction. Principle component analysis (PCA) was conducted to analyze the relationships among target PAHs. Hl-PAHs inventory values were calculated as summations of Cl- and Br-PAHs values because each of these molecule types alone had low detection rates.

3. Results

3.1. Vertical distribution of PAHs

Target PAHs were detected in all samples, while Cl-PAHs were detected in only 67% of the total samples, and in only 19% of the samples within Korea (Fig. 2a). Concentrations of PAHs, e-PAHs, Cl-PAHs, and Br-PAHs ranged from 27 to 6065 ng g^{-1} dw (mean: 506 ng g^{-1} dw), 4.0 to 1002 ng g^{-1} dw (mean: 59 ng g^{-1} dw), from below the MDL to 47 ng g^{-1} dw (mean: 2.6 ng g^{-1} dw), and 3.6 to 2620 ng g^{-1} dw (mean: 56 ng g^{-1} dw), respectively. The sites were grouped based on land use types and divided into industry and municipality and agricultural and aquaculture (Fig. S2). The concentrations of all target PAHs from sites in the industry and municipality divisions were significantly

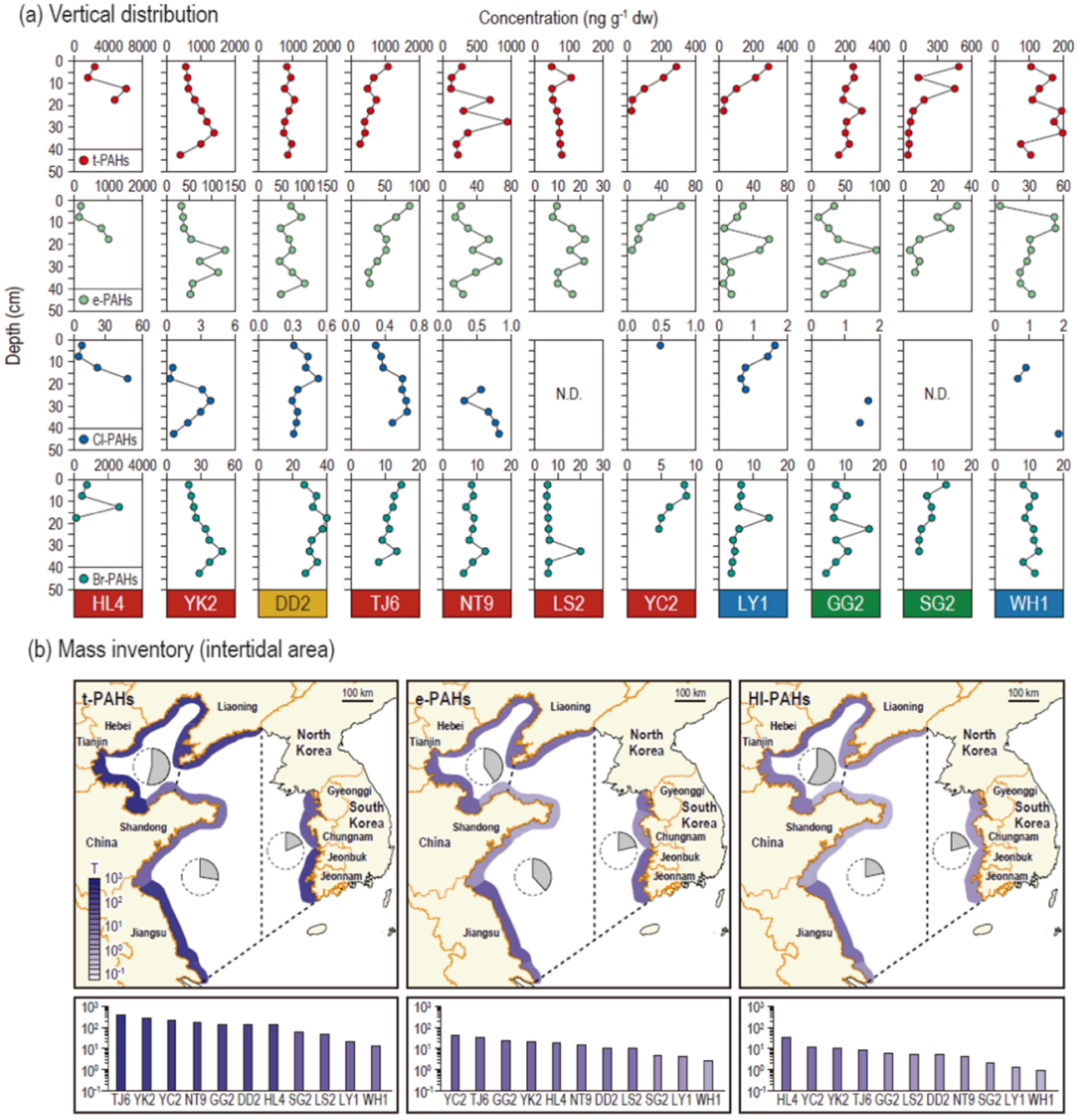

Fig. 2. **(a)** Vertical distributions and **(b)** mass inventory of t-PAHs, e-PAHs, and Hl-PAHs (Cl-PAHs and Br-PAHs) in the intertidal zone of the Yellow and Bohai seas. Circles represent the contributions of the Yellow Sea of Korea, Yellow Sea of China, and Bohai Sea to the total inventory of t-PAHs, e-PAHs, and Hl-PAHs, respectively.

higher than those from sites in the aquaculture and agriculture divisions ($p < 0.01$) (Fig. S3).

The mass inventory of target PAHs in YSLME tidal flats varied among regional areas (Fig. 2b). The mass inventory of t-PAHs, e-PAHs, and Hl-PAHs ranged from 49.4 to 400 t, 4.87 to 41.6 t, and 0.97 to 35.0 t, respectively, accounting for 85.3%, 9.9%, and 4.8% of the total, respectively. Relatively high mass inventories of target PAHs were found in TJ6, YC2, and HL4, respectively.

Eighty-year temporal trends were similar across the YSLME regions. In general, the concentrations of all target PAHs increased gradually over the 80 years, with the highest concentrations occurring in recent years (Fig. 3). Furthermore, concentrations of target PAHs correlated significantly ($p < 0.01$), indicating similar transport and fate patterns.

3.2. Composition and sources of PAHs

The historical trends of all target PAHs, categorized based on ring number, were separated into two groups. High molecular weight (HMW) t-PAHs were present at higher concentrations than low molecular weight (LMW) t-PAHs, and HMW t-PAH concentrations also increased more over time. Particularly high increases in 5- and 6-ring t-PAH concentrations were observed from the 1980s onward. Similarly, HMW e-PAH concentrations showed notable increases after the 1980s. For Hl-PAHs, LMW Hl-PAHs were predominant from past to present. However, HMW-Br-PAHs were only recently detected (within 40 years) in TJ6 and DD2, which had great concentrations of Br-PAHs, similar to the trend observed for other PAHs.

The compositional profiles of all target PAHs were confirmed (Fig. 4a). In t-PAHs, 4-ring PAHs such as fluoranthene (Fl) and pyrene (Py) were dominated (50%), followed by 3-ring (23%), 6-ring (15%), and 5-ring t-PAHs (12%). The proportion of HMW (4–6 rings) in YC2 and SG2 was relatively higher after the 1980s (79%) compared to before the 1980s (60%). Similarly, since the 1980s, the mean composition of HMW t-PAHs in the TJ6 and DD2 was 81%. Similar to t-PAHs, 4-ring e-PAHs constituted the majority (70%) of the e-PAH present, followed by 5-ring (23%) and 3-ring (7%) e-PAHs. However, unlike the trend observed for t-PAHs, the LMW composition of e-PAHs increased after the 1980s. The primary compound in e-PAHs was 11*H*-benzo[*b*]fluorene (11BF) (38%), followed by BBNF (28%), benzo[*e*]pyrene (BEP) (12%), benzo[*j*]fluoranthene (BJF) (11%), and 2-methyl-anthracene (2MA) (5.7%). Among Hl-PAHs, LMW Hl-PAHs predominated in both the Cl-PAHs (100%) and Br-PAHs (96%) classes of Hl-PAHs; this pattern can be attributed to the low observation frequency of HMW Cl-PAHs and Br-PAHs (Fig. 4a). The Cl-PAHs with the lowest MDL, namely 9,10-Cl-Phe, was detected with a detection frequency of 66.6%. The Br-PAHs, 9-bromofluorene (9-Br-Flu) was found in all samples, whereas the observation frequency of other Br-PAH compounds was below 40%. 6-Bromobenzo[*a*]pyrene was the second most dominant compound and was present predominantly at sampling sites within industrial areas, such as TJ6.

The Q_{True}/Q_{Exp} quotient value obtained in the PMF model ranged from 1.26 to 1.0 (Fig. S4). Large decreases were reported for three factors, suggesting that these three factors were appropriate markers to examine (Crilley et al., 2017). The contribution of each source exhibited dissimilar trends over time and region (Fig. 4b). The first source was characterized by 11BF, an indicator of diesel combustion (Wang et al., 2003; Wei et al., 2015). The second source was associated with Ace, fluorene, 2MA, Phe, and anthracene, compounds that are indicative of biomass combustion (McGrath et al., 2001; Ravindra et al., 2008). A third source was predominated by BBNF, indeno[1,2,3-*cd*]pyrene (IcdP), benzo[*g,h,i*]perylene (BghiP), dibenz[*a,h*]anthracene (DbahA), BaP, and benzo[*b*]fluoranthene (BbF), indicating coal and gasoline combustion (Harrison et al., 1996; Ravindra et al., 2008).

3.3. Evaluation of toxic potency of PAHs

The TEQs of t-PAHs were generally higher than those of other PAHs (Fig. S5). The TEQs of t-PAHs, e-PAHs, Cl-PAHs, and Br-PAHs ranged from 101 to 7038 pg-TEQ g^{-1} (mean: 2807 pg-TEQ g^{-1}), 0.1 to 1.4 pg-TEQ g^{-1} (mean: 0.6 pg-TEQ g^{-1}), 0.1 to 0.3 pg-TEQ g^{-1} (mean: 0.2 pg-TEQ g^{-1}), and 0.03 to 6.9 pg-TEQ g^{-1} (mean: 0.9 pg-TEQ g^{-1}), respectively. The mean TEQ concentration of t-PAHs was 3300–12000 times higher than that of other PAHs, due to large-magnitude ReP values

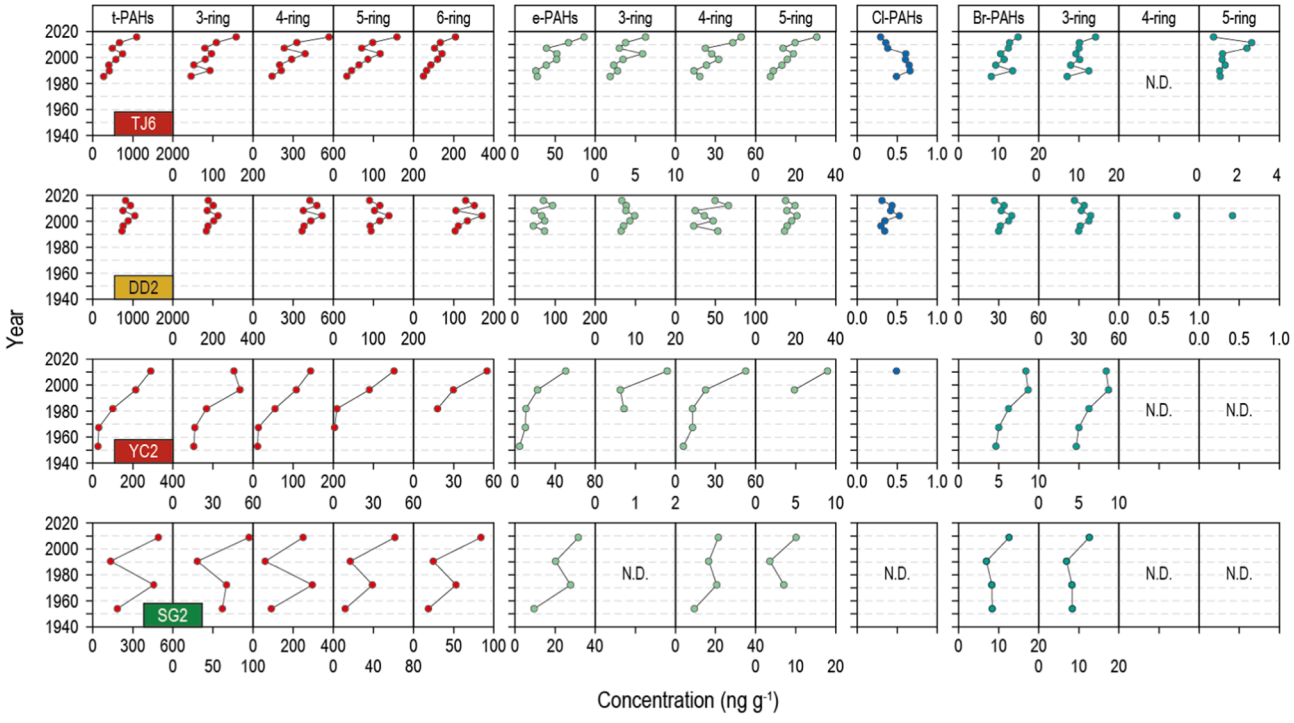

Fig. 3. Historical distribution of t-PAHs, e-PAHs, Cl-PAHs, and Br-PAHs in intertidal sediment cores collected from the Yellow and Bohai seas. N.D. in the blank means not detected.

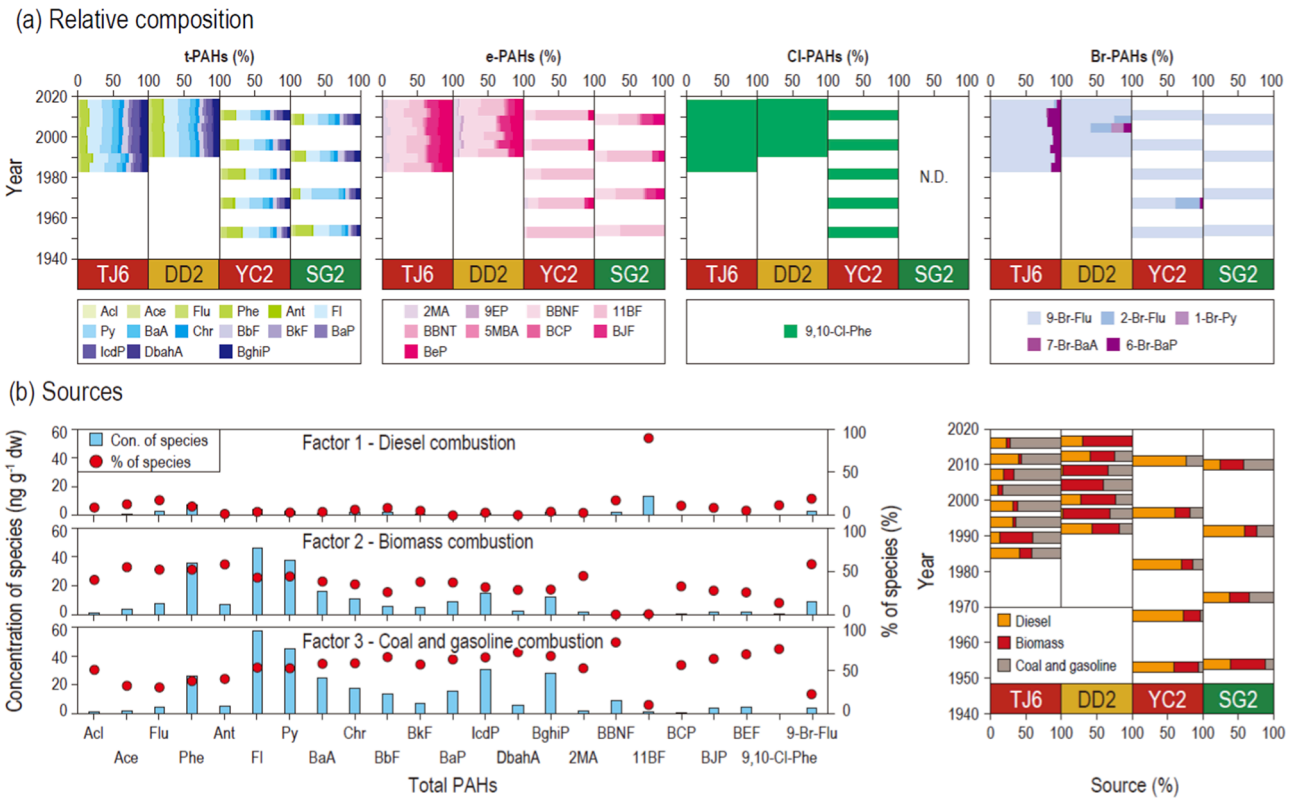

Fig. 4. **(a)** Relative compositions of t-PAHs, e-PAHs, Cl-PAHs, and Br-PAHs in intertidal sediment cores collected from the Yellow and Bohai seas. N.D. in the blank means not detected. **(b)** Sources derived from a PMF receptor model of all target PAHs in intertidal sediment cores collected from the Yellow and Bohai seas.

and t-PAH concentrations (Table S3).

TEQs were dominated by t-PAHs, which accounted for over 99% of the total TEQs at all sites and periods (Fig. S5 and Table S3). Chrysene (Chr) had the highest contribution (45%), followed by benzo[*a*] anthracene (BaA) (36%), BaP (15%), and Py (2.6%). The substantial presence of these molecules reflects their RePs. 7-Bromobenz[*a*] anthracene (7-Br-BaA) accounted for 89% of observed Br-PAHs, with the next dominant molecules being 1-bromopyrene (1-Br-Py) (6%) and 2-bromofluorene (2-Br-Flu) (4%).

4. Discussion

4.1. Temporal trends of PAHs contamination

The vertical distribution of target PAHs was divided by land-use types, with the HL4 showing the highest PAHs concentration and being distinct from other sites. PAH concentrations were higher in stations located within industrial and municipal regions (YK2, DD2, TJ6, and NT9) than in stations within agricultural and aquaculture (other sites) regions. Previous studies have reported relatively high contamination levels in surface sediments at Huludao (HL4), Yingkou (YK2), Dandong (DD2), and Nantong (NT9) (Zheng et al., 2008; Luo et al., 2012; Wang et al., 2013; Tian et al., 2020; Yoon et al., 2020), indicating that contamination in these regions has persisted with potential contributions from multiple land use types.

The greatest mass inventory of target PAHs was found in the Bohai Sea, followed by the Yellow Sea of China and the Yellow Sea of Korea. The intertidal area at site HL4 had the lowest in the entire region. However, this sampling site had the highest mass inventory of Hl-PAHs observed. This high mass inventory result can be attributed to Hl-PAH concentrations in HL4 being 30 to 150 times higher compared to those in the other regions, indicating severe contamination. Of note, relatively high mass inventories were observed at the YK2, HL4, and TJ6, all of which are located along the Bohai Sea. In addition, the mass inventory of all target PAHs was highest from the Bohai Sea. Thus, despite region-specific trends, general trends in the sea area were observed to be similar.

Temporal trends observed in our study were consistent with previous research (Yan et al., 2009; Liu et al., 2012; Ma et al., 2018, 2020; Wang et al., 2020) in terms of reflecting changes associated with changes in GDP, rural population, and fossil fuel consumption in Korea and China (Fig. S6). Relatively low PAH concentrations had been observed in South Korea until the early 1960s, coinciding with the pre-industrialization period (before 1961). Subsequently, concentrations increased in association with the continuous development that had occurred in the region from 1962 (economic development plan) to the present. In the SG2 sampling site region, an estuary dam was constructed in the 1970s, and a nearby industrial complex was developed in the mid-1990s. The historical trends of all target PAHs in SG2 reflect these activities well.

The moderate increase in PAH concentrations that occurred in China until the mid-1970s can be attributed to a series of geopolitical circumstances, including slowed development caused by World War II (1937–1945), the Chinese Civil War (1946–1949), and the Cultural Revolution (1966–1976). After the 1970s, a continuously increasing PAH concentration seemed to be driven by rapid development, following the enforcement of the Reform and Open Policy in 1978. Since the 2000s, PAH concentrations have increased slowly while energy consumption has risen rapidly likely owing to initiatives regulating emissions (e.g., atmospheric emissions of dioxin) and increased environmental protection (Guo et al., 2013a; MOE, 2014; Cai et al., 2016; Kim et al., 2019b, Wang et al., 2020). Recently, Ma et al. (2020) reported comparable results that demonstrate the positive effects of environmental awareness, including emission guidelines (Tang et al., 2015). Despite these efforts, PAH concentrations increased during the 2000s at some sites, indicating the need for regional environmental management in contaminated areas and controlling non-point sources.

4.2. Potential sources of PAHs based on molecular compositions

The compositional profiles of t-PAHs suggested a change in their major source since the 1980s in both Korea and China. The composition of perylene, an indicator of pyrolytic, petrogenic, and diagenetic origin, varied across sites and core depths (Venkatesan, 1988). Generally, the vertical distribution of perylene comprised less than 10% of the total concentration and accounted for over 10% of 5-ring t-PAH concentrations (Fig. S7), indicating pyrolytic origin (Baumard et al., 1998). Meanwhile, the substantial presence of perylene at the DD2 indicated that there had been major inputs of terrestrial organic matter (Baumard et al., 1998).

The compositional profiles of e-PAHs indicated that coal tar combustion and fossil fuel emissions were likely major e-PAH sources (Koganti et al., 2000; Wang et al., 2003). In addition, relatively high compositions of LMW (especially 2MA) and 5-ring e-PAHs (including BEP and BJF) were found at the TJ6 and DD2, where relatively high concentrations of e-PAHs were found. Thus, wood combustion, diesel combustion, and vehicle emissions represented primary e-PAH sources at TJ6 and DD2 (Rogge et al., 1993; Larsen and Baker, 2003).

The compositional profiles of Cl-PAHs in this study differed from those reported in previous studies in which 9,10-Cl-Phe accounted for less than 10% of the total composition (Horii et al., 2009b; Ohura et al., 2015). Several Hl-PAHs were detected only at YK2 and HL4. For instance, 1-chloropyrene (1-Cl-Py) was the dominant congener in HL4, which is consistent with previous findings (Horii et al., 2009b; Ohura et al., 2015). 9-Br-Flu accounted for 81% of Br-PAH concentrations in sediments at Tokyo Bay in previous data, which is consistent with our findings (Sei et al., 2021). 6-Bromobenzo[*a*]pyrene exhibited little temporal change in only industrial areas. Thus, Br-PAHs mainly originate from regional industrial areas (Ohura et al., 2009). Previously, Vuong et al. (2020a) reported that brominated-Flu and chlorinated-Phe were the major contaminants present at sites impacted by industrial cities. Furthermore, we obtained Hl-PAH congeners ratio values that were similar to those reported in sites affected by waste incinerators, secondary copper smelting, cement kiln co-processing solid waste, and road tunnels (Table S4).

The three PAH sources showed different trends. Diesel combustion was found primarily in regions with relatively low concentrations of target PAHs. The contribution from each site was similar to that in 1950, indicating that the impact remained stable over 80 years. Biomass combustion had the most profound contribution at DD2, and this distinction remained true for over 80 years. The substantial contribution of biomass could be attributed to household energy usage until recently (Zhang et al., 2007). Coal and gasoline combustion, which generated the most pronounced contribution at TJ6 (industrial land use), increased gradually over the 80-year period in all sites, reflecting an increase in coal and gasoline usage (Fig. S6). Overall, over the last 80 years, the contribution of diesel and biomass combustion varied with respect to region and land use, while the contribution of coal and gasoline combustion increased in all regions.

4.3. Potential toxicity of t-PAHs, e-PAHs, and Hl-PAHs

The TEQs of t-PAHs in this study were generally lower compared to previously reported values for core sediments. The TEQs in this study were about 2–10 times lower compared to those in Kaohsiung Harbor (Dong et al., 2014; Chen et al., 2016), Wuhan Lake (Lu et al., 2015), and Hongfeng Lake (Guo et al., 2011), but were about eight times higher than those reported for Daliao River (Guo et al., 2013b). Regarding Hl-PAHs, TEQ trends differed between Cl-PAHs and Br-PAHs in previous studies in which surface sediment material was examined. The TEQ of Cl-PAHs in this study was 120 times lower than that recorded in the Maozhou River (Sun et al., 2012), but it was similar to that in Tokyo Bay (Sei et al., 2021). For Br-PAHs, the TEQ was 84 times lower compared to that in Maozhou River, but was similar to that in Tokyo Bay. Overall, the potential toxicity was relatively low, but the YSLME was contaminated with Hl-PAHs, indicating that further source tracking and monitoring are necessary.

The present results fit well with previously published results reported by Sun et al. (2012), indicating that Hl-PAHs contributed less than 10% to the total TEQs in the Maozhou River. However, Hl-PAHs have been observed at substantial levels in atmospheric samples (Vuong et al., 2020a). These contrasting results may be attributed to the rapid decomposition of Hl-PAHs in environments (Ohura et al., 2009) or to congeners known to have a relatively high ReP not being analyzed in this study. In the future, additional congeners analyses and toxicity testing are necessary to obtain more accurate measures of the potential toxicity of traditional PAHs with substituted- and Hl-PAHs in marine environments.

4.4. Comparison to previous studies

The historical records of t-PAHs in the current study were compared with previous data recorded for the Yellow Sea, Bohai Sea, East China Sea, and South China Sea. Because only one prior study evaluated Cl-PAHs in vertical sediment in the Yellow Sea, only t-PAHs were compared (Liu et al., 2005; Guo et al., 2006; Guo et al., 2007; Yan et al., 2009; Zhang et al., 2009; Hu et al., 2011; Liu et al., 2012; Zhang et al., 2013; Li et al., 2015; Cai et al., 2016) (Fig. 5). The concentrations of t-PAHs in the entire region have increased significantly ($p < 0.01$), with a relatively faster increase in intertidal areas and slower increase in subtidal areas. Relatively low t-PAH concentrations have been reported previously, likely due to sediment cores being collected from the subtidal zones of estuaries, bays, coasts, and offshore areas. However, a relatively high t-PAH concentration was reported from the intertidal area (Zhang et al., 2013), indicating that there is contamination of the intertidal area. Concentrations of t-PAHs did not differ significantly in all areas, suggesting that there is a continuous t-PAH increase in the YSLME and surrounding waters, with this trend noticeably accelerating in the intertidal zone.

Spatial and temporal variations were observed in the relative composition of t-PAHs in the YSLME (Fig. 6a). The intertidal zone has been shown to have a predominance of HMW t-PAHs, while LMW t-PAHs have been found to be more abundant in coastal and offshore areas (Hu et al., 2011; Zhang et al., 2009, Zhang et al., 2013). HMW PAHs precipitate near their sources and do not migrate far, whereas volatile LMW PAHs can be transported more readily to coastal and offshore areas before being deposited (Wania and Mackay, 1996). The proportion of HMW t-PAHs has increased in recent decades, indicating that fossil fuel combustion is producing toxic t-PAHs contamination. A PCA result from coastal and offshore areas showed similar composition profiles regardless of sea area, while the intertidal zone exhibited variation in t-PAH proportion with respect to both region and time, likely due to direct inputs from a complex and dynamic environment. In contrast, coastal and offshore areas had indirect PAH inputs and were relatively more stable.

4.5. Deposition flux and mass inventory of PAHs

The deposition flux observed in the current study was comparable to or higher than the fluxes reported in previous studies (Table 1). The deposition flux in this study was similar to that documented in the Rhone Delta (Tolosa et al., 1996), East China Sea (Lin et al., 2013), Changjiang Estuary (Wang et al., 2016), Changjiang Delta, and Zhejiang-Fujian coast (Wang et al., 2017). In contrast, the deposition flux was higher than that recorded in the Ebro delta (Tolosa et al., 1996), Proximal Rhone delta, Distal Rhone delta (Bouloubassi et al., 2012), Pearl Estuary (Chen et al., 2006), Beibu Gulf (Li et al., 2015), and Gulf of Thailand (Hu et al., 2017).

The t-PAHs deposition flux in coastal and offshore areas of the Bohai Sea has been reported to be in the range of 51–385 ng cm^{-2} y^{-1} (Qin

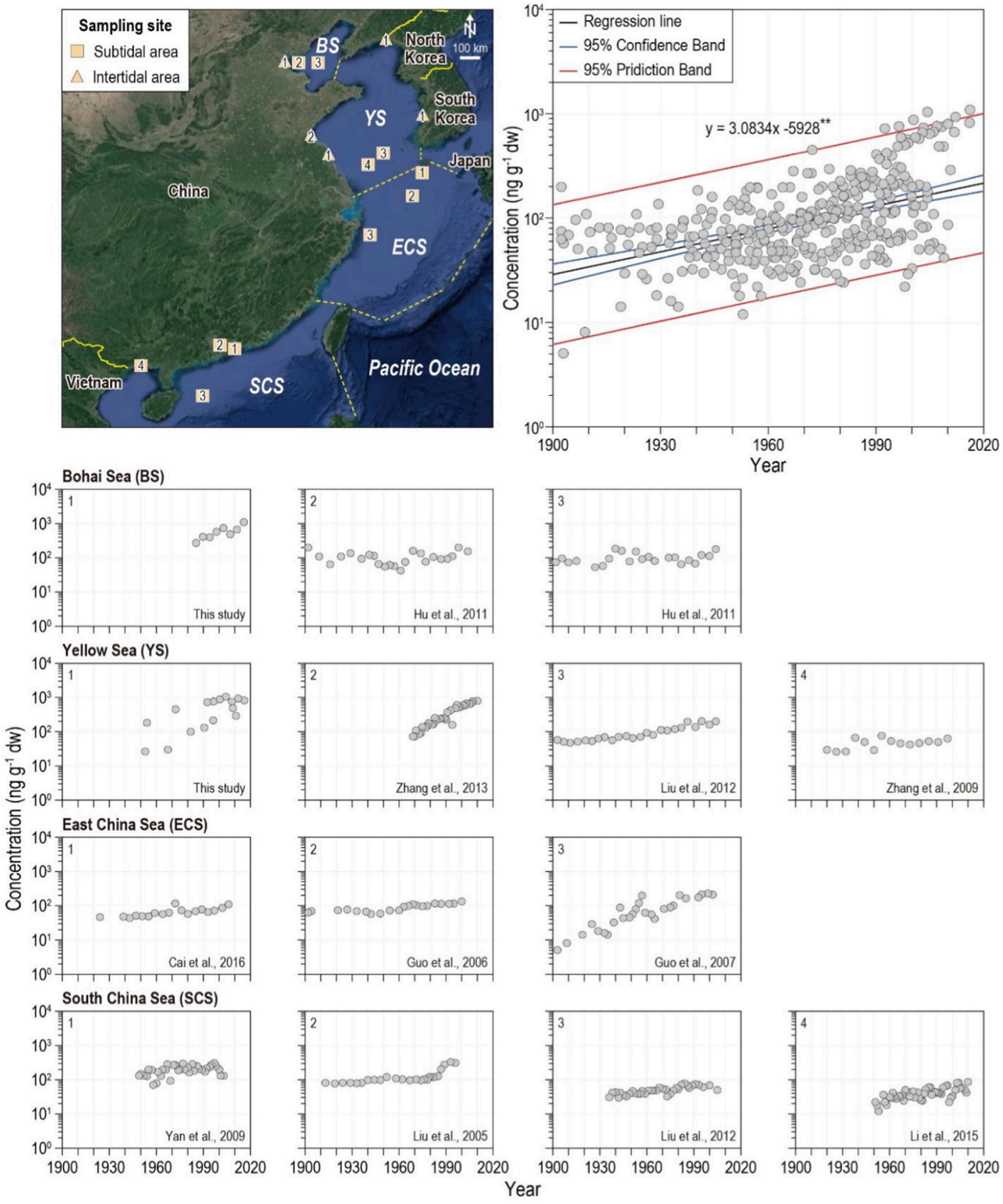

Fig. 5. Mini review of studies investigating historical deposition of t-PAHs in the Yellow, Bohai, East China, and South China seas.

et al., 2011; Wang et al., 2017). However, the t-PAH deposition flux in the tidal flat of the Bohai Sea in this study was 1330 ng cm^{-2} y^{-1}, which is about 4–26 times higher than flux values observed in coastal and offshore areas. Furthermore, the deposition flux in this study was similar to 10 times higher (102–1624 ng cm^{-2} y^{-1}) than previous records from coastal areas in the central Yellow Sea (71–162 ng cm^{-2} y^{-1}) (Liu et al., 2012; Wang et al., 2017). Of note, assuming that only terrestrial inputs affect t-PAH deposition flux, it can be deduced that about 83%, 10%, and 7% of t-PAHs are introduced and accumulated in the intertidal zone, coastal, and offshore areas, respectively (Fig. 6b). Therefore, the intertidal zone may serve as a buffer zone for marine pollution and play an important role in preventing contamination on coasts and offshore.

The mass inventory found in the present study was comparable to or higher than the mass inventory values reported in previous studies

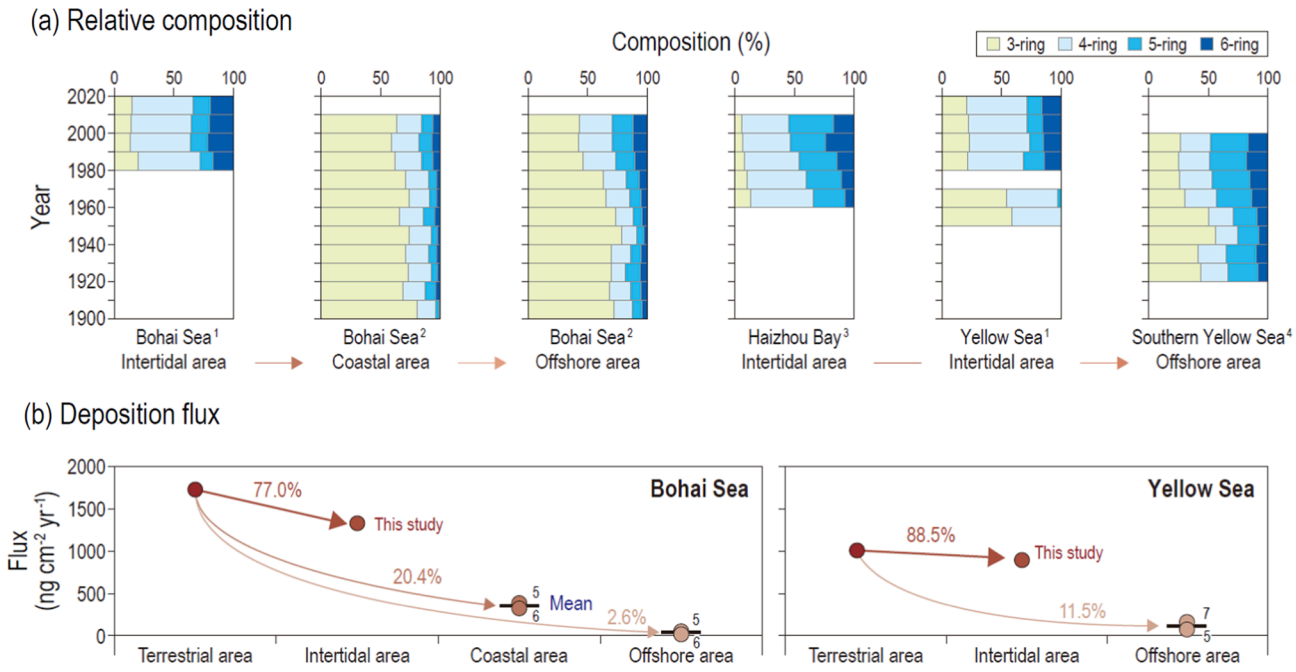

Fig. 6. (a) Relative compositions and (b) deposition flux of t-PAHs from terrestrial to offshore areas in the Yellow and Bohai seas ([1] This study; [2] Hu et al., 2011; [3] Zhang et al., 2013; [4] Zhang et al., 2009; [5] Wang et al., 2017; [6] Qin et al., 2011; [7] Liu et al., 2012).

Table 1
Comparison of the mean deposition flux per unit area of t-PAHs in sediment collected from pro-deltas, estuaries, bays, and seas for Korea and China.

Region	Sediment type	Chemical	Sampling year	Deposition flux(ng cm^{-2} y^{-1})	Reference
Rhone prodelta	Surface	15PAHs	1987–1991	1067	Tolosa et al. (1996)
Ebro prodelta	Surface	15PAHs	1987–1991	39	Tolosa et al. (1996)
Proximal Rhone prodelta	Surface	21PAHs	2001	28	Bouloubassi et al. (2012)
Distal Rhone prodelta	Surface	21PAHs	2001	0.2	
Pearl Estuary	Surface	25PAHs	2002	20	Chen et al. (2006)
Bohai Sea	Surface	16PAHs	2006	85	Qin et al. (2011)
East China Sea	Surface	16PAHs	2006–2007	155	Lin et al. (2013)
Yellow Sea	Core	16PAHs	2007	162	Liu et al. (2012)
Beibu Gulf, China	Core	15PAHs	2010	74.8	Li et al. (2015)
Gulf of Thailand	Surface	16PAHs	2010–2012	4.2	Hu et al. (2017)
Changjiang Estuary	Surface	16PAHs	2013	219	Wang et al. (2016)
Western Bohai Sea	Surface	16PAHs	2013	385	Wang et al. (2017)
Open Bohai Sea	Surface	16PAHs	2013	51	
Central Yellow Sea	Surface	16PAHs	2013	71	
Changjiang Delta mud area	Surface	16PAHs	2013	219	
Zhejiang-Fujian coast	Surface	16PAHs	2013	166	
Bohai Bay (TJ6) [a]	Core	15PAHs	2018	1330	This study
Korea Bay (DD2) [a]	Core	15PAHs	2018	1624	
Yancheng Coast (YC2) [a]	Core	15PAHs	2018	102	
Asan Bay (SG2) [a]	Core	15PAHs	2018	105	

[a] Sediment core was collected in the intertidal zone.

(Table 2). The mass inventory of the YSLME was similar to that recorded for the Peral River Estuary, the northern part of the South China Sea (Chen et al., 2006), and Central Beibu Gulf. In contrast, the mass inventory recorded in this study was higher than that reported for the Beibu Gulf (Li et al., 2015), Pearl River Estuary (Pintado-Herrera et al., 2017), Nanliu Mangrove, and Chinese Mangroves (Kaiser et al., 2016). However, the mass inventory per unit area (kg cm^{-1} km^{-2}), which normalizes for the difference in the area and depth, was relatively higher in the present study than in most previous studies, with the exception of that reported for the Pearl River Estuary (Chen et al., 2006). The present data thus suggest that the benthic environment in the YSLME is likely to be severely polluted. Overall, t-PAH concentration, deposition flux, and mass inventory values were greater in the YSLME compared to neighboring areas, underscoring a need for continued monitoring.

5. Conclusions

The present study provided novel historical information on the deposition, mass inventory, sources, toxic potency, and deposition flux of t-PAHs, e-PAHs, Cl-PAHs, and Br-PAHs on the LME scale. Historical trends of target PAHs reflected the development and social state evolution of Korea and China over the last 80 years. In addition, temporal change in sources and regional differences of flux and inventory were recorded in all regions. The presently observed t-PAHs concentration, deposition flux, and mass inventory data values were higher in this study than in previous studies performed in the YSLME. It was challenging to evaluate temporal changes to e-PAHs and Hl-PAHs due to there being insufficient data on historical trends in marine environments worldwide. This study presents the first historical assessment of e-PAHs, Cl-PAHs, and Br-PAHs in marine ecosystems on the LME scale (for Korea and

Table 2
Comparison of the mass inventory of t-PAHs in sediment collected from estuaries, bays, and seas for Korea and China.

Region	Sedimenttype	Area (km^2)	Depth (cm)	Mass inventory (t)	Mass inventoryper unit area (kg cm^{-1} km^{-2})	Reference
Pearl River Estuary	Surface	2016	5	126[b]	12.5	Chen et al. (2006)
Northern South China Sea	Surface	21,337	5	423[b]	4.0	
Beibu Gulf	Surface	400	5	2 [b]	1.0	Li et al. (2015)
Pearl River Estuary	Surface	3295	5	50[c]	3.0	Pintado-Herrera et al. (2017)
Central Beibu Gulf	Core	40,000	35	1127[c]	0.8	Kaiser et al. (2016)
Nanliu Mangrove [a]	Core	5	60	0.07–0.24[c]	0.2–0.8	
Chinese Mangroves [a]	Core	208	60	0.89–11.73[c]	0.1–0.9	
Yellow Sea (Korea) [a]	Core	1715	50	245[c]	2.9	This study
Yellow Sea (China) [a]	Core	2532	50	716[c]	5.7	
Bohai Sea [a]	Core	1010	50	602[c]	11.9	

[a] Sediment core was collected in the intertidal zone.
[b] Mass inventory was calculated using the concentrations of 25 PAHs.
[c] Mass inventory was calculated using the concentrations of 15 PAHs.

China), which is crucial for identifying major sources. Such information could be used to calculate deposition fluxes and mass inventory, allowing the establishment of future management of emerging PTSs. Overall, our findings provide novel knowledge on the history of coastal PAH pollution from the past to the present, which will be valuable for future monitoring strategies and pollution control policies.

CRediT authorship contribution statement

Seo Joon Yoon: Conceptualization, Formal analysis, Visualization, Writing – original draft. **Seongjin Hong:** Conceptualization, Visualization, Project administration, Funding acquisition, Writing – review & editing. **Junghyun Lee:** Investigation, Formal analysis, Visualization. **Jongmin Lee:** Investigation, Formal analysis. **Youngnam Kim:** Formal analysis. **Moo Joon Lee:** Investigation. **Jongseong Ryu:** Investigation, Project administration. **Kyungsik Choi:** Investigation, Project administration. **Bong-Oh Kwon:** Investigation, Project administration. **Wenyou Hu:** Investigation, Project administration. **Tieyu Wang:** Investigation, Project administration. **Jong Seong Khim:** Conceptualization, Investigation, Project administration, Funding acquisition, Supervision, Writing – review & editing.

Declaration of Competing Interest

The authors declare that they have no known competing financial interests or personal relationships that could have appeared to influence the work reported in this paper.

Data availability

Data will be made available on request.

Acknowledgments

This work was supported by the projects entitled “Integrated Management of Marine Environment and Ecosystems Around Saemangeum (20140257)” and “Development of Source Identification and Apportionment Methods for Toxic Substances in Marine Environments (20220534)” programs of Korea institute of Marine Science & Technology Promotion (KIMST) funded by the Ministry of Oceans and Fisheries. This study was also supported by the National Research Foundation grants funded by the Korean Government (2021R1C1C1005977, 2021R1I1A1A01049680, and 2022R1I1A1A01073054).

Appendix A. Supplementary material

Supplementary data to this article can be found online at https://doi.org/10.1016/j.envint.2023.108037.

References

An, Y., Hong, S., Yoon, S.J., Cha, J., Shin, K.-H., Khim, J.S., 2020. Current contamination status of traditional and emerging persistent toxic substances in the sediments of Ulsan Bay. South Korea. Mar. Pollut. Bull. 160, 111560 https://doi.org/10.1016/j.marpolbul.2020.111560.

Avnimelech, Y., Ritvo, G., Meijer, L.E., Kochba, M., 2001. Water content, organic carbon and dry bulk density in flooded sediment. Aquac. Eng. 25, 25–33. https://doi.org/10.1016/S0144-8609(01)00068-1.

Baumard, P., Budzinski, H., Michon, Q., Garrigues, P., Burgeot, T., Bellocq, J., 1998. Origin and bioavailability of PAHs in the Mediterranean Sea from mussel and sediment records. Estuar. Coast. Shelf Sci. 47, 77–90. https://doi.org/10.1006/ecss.1998.0337.

Benner, B.A., Wise, S.A., Currie, L.A., Klouda, G.A., Klinedinst, D.B., Zweidinger, R.B., Stevens, R.K., Lewis, C.W., 1995. Distinguishing the contributions of residential wood combustion and mobile source emissions using relative concentrations of dimethylphenanthrene isomers. Environ. Sci. Technol. 29, 2382–2389. https://doi.org/10.1021/es00009a034.

Bouloubassi, I., Roussiez, V., Azzoug, M., Lorre, A., 2012. Sources, dispersal pathways and mass budget of sedimentary polycyclic aromatic hydrocarbons (PAH) in the NW Mediterranean margin, Gulf of Lions. Mar. Chem. 142, 18–28. https://doi.org/10.1016/j.marchem.2012.07.003.

Cai, Y., Wang, X., Wu, Y., Li, Y., Ya, M., 2016. Over 100-year sedimentary record of polycyclic aromatic hydrocarbons (PAHs) and organochlorine compounds (OCs) in the continental shelf of the East China Sea. Environ. Pollut. 219, 774–784. https://doi.org/10.1016/j.envpol.2016.07.053.

Cha, J., Hong, S., Kim, J., Lee, J., Yoon, S.J., Lee, S., Moon, H.-B., Shin, K.-H., Hur, J., Giesy, J.P., 2019. Major AhR-active chemicals in sediments of Lake Sihwa, South Korea: Application of effect-directed analysis combined with full-scan screening analysis. Environ. Int. 133, 105199 https://doi.org/10.1016/j.envint.2019.105199.

Chen, C.-F., Chen, C.-W., Ju, Y.-R., Dong, C.-D., 2016. Vertical profile, source apportionment, and toxicity of PAHs in sediment cores of a wharf near the coal-based steel refining industrial zone in Kaohsiung, Taiwan. Environ. Sci. Pollut. Res. 23, 4786–4796. https://doi.org/10.1007/s11356-015-5716-8.

Chen, S.-J., Luo, X.-J., Mai, B.-X., Sheng, G.-Y., Fu, J.-M., Zeng, E.Y., 2006. Distribution and mass inventories of polycyclic aromatic hydrocarbons and organochlorine pesticides in sediments of the Pearl River Estuary and the northern South China Sea. Environ. Sci. Technol. 40, 709–714. https://doi.org/10.1021/es052060g.

Cho, J., Hyun, S., Han, J.H., Kim, S., Shin, D.H., 2015. Historical trend in heavy metal pollution in core sediments from the Masan Bay. Korea. Mar. Pollut. Bull. 95, 427–432. https://doi.org/10.1016/j.marpolbul.2015.03.034.

Crilley, L.R., Lucarelli, F., Bloss, W.J., Harrison, R.M., Beddows, D.C., Calzolai, G., Nava, S., Valli, G., Bernardoni, V., Vecchi, R., 2017. Source apportionment of fine and coarse particles at a roadside and urban background site in London during the 2012 summer ClearfLo campaign. Environ. Pollut. 220, 766–778. https://doi.org/10.1016/j.envpol.2016.06.002.

Crozaz, G., Picciotto, E., De Breuck, W., 1964. Antarctic snow chronology with Pb210. J. Geophys. Res. 69, 2597–2604. https://doi.org/10.1029/JZ069i012p02597.

Dong, C.-D., Chen, C.-F., Chen, C.-W., 2014. Vertical profile, sources, and equivalent toxicity of polycyclic aromatic hydrocarbons in sediment cores from the river mouths of Kaohsiung Harbor. Taiwan. Mar. Pollut. Bull. 85, 665–671. https://doi.org/10.1016/j.marpolbul.2013.09.037.

Fu, P.P., Von Tungeln, L.S., Zhan, D.-J., Bucci, T., 1996. Potent tumorigenicity of 7-chlorobenz[a]anthracene and 7-bromobenz[a]anthracene in the neonatal B6C3F1

male mouse. Cancer Lett. 101, 37–42. https://doi.org/10.1016/0304-3835(96)04111-0.
Fu, P.P., Von Tungeln, L.S., Chiu, L.-H., Own, Z.Y., 1999. Halogenated-polycyclic aromatic hydrocarbons: A class of genotoxic environmental pollutants. Environ. Carcino. & Ecotox. Rev. C17 (2), 71–109. https://doi.org/10.1080/10590509909373510.
Fujima, S., Ohura, T., Amagai, T., 2006. Simultaneous determination of gaseous and particulate chlorinated polycyclic aromatic hydrocarbons in emissions from the scorching of polyvinylidene chloride film. Chemosphere 65, 1983–1989. https://doi.org/10.1016/j.chemosphere.2006.07.003.
Gibson, T.L., Smart, V.B., Smith, L.L., 1978. Non-enzymic activation of polycyclic aromatic hydrocarbons as mutagens. Mutat. Res. Mol. Mut. 49, 153–161. https://doi.org/10.1016/0027-5107(78)90152-5.
Guerra, R., Pasteris, A., Righi, S., Ok, G., 2019. Historical record of polychlorinated biphenyls (PCBs) in the continental shelf of the Korea Strait. Chemosphere 237, 124438. https://doi.org/10.1016/j.chemosphere.2019.124438.
Guo, J., Costa Jr, O.S., Wang, Y., Lin, W., Wang, S., Zhang, B., Cui, Y., Fu, H., Zhang, L., 2020. Accumulation rates and chronologies from depth profiles of 210Pbex and 137Cs in sediments of northern Beibu Gulf. South China sea. J. Environ. Radioact. 213, 106136 https://doi.org/10.1016/j.jenvrad.2019.106136.
Guo, W., He, M., Yang, Z., Zhang, H., Lin, C., Tian, Z., 2013b. The distribution, sources and toxicity risks of polycyclic aromatic hydrocarbons and n-alkanes in riverine and estuarine core sediments from the Daliao River watershed. Environ. Earth Sci. 68, 2015–2024. https://doi.org/10.1007/s12665-012-1889-3.
Guo, Z., Lin, T., Zhang, G., Yang, Z., Fang, M., 2006. High-resolution depositional records of polycyclic aromatic hydrocarbons in the central continental shelf mud of the East China Sea. Environ. Sci. Technol. 40, 5304–5311. https://doi.org/10.1021/es060878b.
Guo, Z.G., Lin, T., Zhang, G., Yang, Z.S., Fang, M., 2007. The sedimentary fluxes of polycyclic aromatic hydrocarbons in the Yangtze River Estuary coastal sea for the past century. Sci. Total Environ. 386, 33–41. https://doi.org/10.1016/j.scitotenv.2007.07.019.
Guo, J.-Y., Wu, F.-C., Zhang, L., Liao, H.-Q., Zhang, R.-Y., Li, W., Zhao, X.-L., Chen, S.-J., Mai, B.-X., 2011. Screening level of PAHs in sediment core from Lake Hongfeng, Southwest China. Arch. Environ. Contam. Toxicol. 60, 590–596. https://doi.org/10.1007/s00244-010-9568-4.
Guo, J.Y., Wu, F.C., Liao, H.Q., Zhao, X.I., Li, W., Wang, J., Wang, L.F., Giesy, J.P., 2013a. Sedimentary record of polycyclic aromatic hydrocarbons and DDTs in Dianchi Lake, an urban lake in Southwest China. Environ. Sci. Pollut. Res. 20 (8), 5471–5480. https://doi.org/10.1007/s11356-013-1562-8.
Gwak, J., Cha, J., Lee, J., Kim, Y., An, S.-A., Lee, S., Moon, H.-B., Hur, J., Giesy, J.P., Hong, S., Khim, J.S., 2022. Effect-directed identification of novel aryl hydrocarbon receptor-active aromatic compounds in coastal sediments collected from a highly industrialized area. Sci. 526 Total Environ. 803, 149969 https://doi.org/10.1016/j.scitotenv.2021.149969.
Harrison, R.M., Smith, D., Luhana, L., 1996. Source apportionment of atmospheric polycyclic aromatic hydrocarbons collected from an urban location in Birmingham, UK. Environ. Sci. Technol. 30, 825–832. https://doi.org/10.1021/es950252d.
Hoagland, P., Jin, D., 2006. Accounting for Economic Activities on Large Marine Ecosystems and Regional Seas. NOAA's Large Marine Ecosystems (LMEs) and UNEP Regional Seas Programme. https://wedocs.unep.org/bitstream/handle/20.500.11822/11814/rsrs181.pdf?sequence=1&amp%3BisAllowed=.
Hong, S., Khim, J.S., Naile, J.E., Park, J., Kwon, B.-O., Wang, T., Lu, Y., Shim, W.J., Jones, P.D., Giesy, J.P., 2012. AhR-mediated potency of sediments and soils in estuarine and coastal areas of the Yellow Sea region: a comparison between Korea and China. Environ. Pollut. 171, 216–225. https://doi.org/10.1016/j.envpol.2012.08.001.
Hong, S., Kim, Y., Lee, Y., Yoon, S.J., Lee, C., Liu, P., Kwon, B.-O., Hu, W., Khim, J.S., 2022. Distributions and potential sources of traditional and emerging polycyclic aromatic hydrocarbons in sediments from the lower reach of the Yangtze River. China. Sci. Total Environ. 152831 https://doi.org/10.1016/j.scitotenv.2021.152831.
Horii, Y., Ok, G., Ohura, T., Kannan, K., 2008. Occurrence and profiles of chlorinated and brominated polycyclic aromatic hydrocarbons in waste incinerators. Environ. Sci. Technol. 42, 1904–1909. https://doi.org/10.1021/es703001f.
Horii, Y., Khim, J.S., Higley, E.B., Giesy, J.P., Ohura, T., Kannan, K., 2009a. Relative potencies of individual chlorinated and brominated polycyclic aromatic hydrocarbons for induction of aryl hydrocarbon receptor-mediated responses. Environ. Sci. Technol. 43, 2159–2165. https://doi.org/10.1021/es8030402.
Horii, Y., Ohura, T., Yamashita, N., Kannan, K., 2009b. Chlorinated polycyclic aromatic hydrocarbons in sediments from industrial areas in Japan and the United States. Arch. Environ. Contam. Toxicol. 57, 651–660. https://doi.org/10.1007/s00244-009-9372-1.
Hu, L., Guo, Z., Shi, X., Qin, Y., Lei, K., Zhang, G., 2011. Temporal trends of aliphatic and polyaromatic hydrocarbons in the Bohai Sea, China: evidence from the sedimentary record. Org. Geochem. 42, 1181–1193. https://doi.org/10.1016/j.orggeochem.2011.08.009.
Hu, L., Shi, X., Qiao, S., Lin, T., Li, Y., Bai, Y., Wu, B., Liu, S., Kornkanitnan, N., Khokiattiwong, S., 2017. Sources and mass inventory of sedimentary polycyclic aromatic hydrocarbons in the Gulf of Thailand: Implications for pathways and energy structure in SE Asia. Sci. Total Environ. 575, 982–995. https://doi.org/10.1016/j.scitotenv.2016.09.158.
Jeddi, M., Karray, F., Battimelli, A., Danel, A., Garali, M.B.S., Tedetti, M., Zaghden, H., Mhiri, N., Sousbie, P., Patureau, D., Sayadi, S., 2022. Biochemical characterization, microbial diversity and biodegradability of coastal sediments in the Gulf of Gabès, Southern Mediterranean Sea. Int. J. Environ. Sci. Technol. 19, 2389–2408. https://doi.org/10.1007/s13762-021-03307-0.
Kaiser, D., Schulz-Bull, D.E., Waniek, J.J., 2016. Profiles and inventories of organic pollutants in sediments from the central Beibu Gulf and its coastal mangroves. Chemosphere 153, 39–47. https://doi.org/10.1016/j.chemosphere.2016.03.041.
Khim, J.S., Hong, S., Yoon, S.J., Nam, J., Ryu, J., Kang, S.-G., 2018a. A comparative review and analysis of tentative ecological quality objectives (EcoQOs) for protection of marine environments in Korea and China. Environ. Pollut. 242, 2027–2039. https://doi.org/10.1016/j.scitotenv.2018.07.169.
Khim, J.S., Park, J., Song, S.J., Yoon, S.J., Noh, J., Hong, S., Kwon, B.-O., Ryu, J., Zhang, X., Wang, T., 2018b. Chemical-, site-, and taxa-dependent benthic community health in coastal areas of the Bohai Sea and northern Yellow Sea: a sediment quality triad approach. Sci. Total Environ. 645, 743–752. https://doi.org/10.1016/j.envpol.2018.06.094.
Kim, E.-K., Barghi, M., Choi, M., Moon, H.-B., 2019a. Spatial and temporal trends of PCDD/Fs in sediment and bivalves along the Korean coasts during 2001–2012. Mar. Pollut. Bull. 146, 183–189. https://doi.org/10.1016/j.marpolbul.2019.06.002.
Kim, J., Hong, S., Cha, J., Lee, J., Kim, T., Lee, S., Moon, H.B., Shin, K.H., Hur, J., Lee, J. S., Giesy, J.P., Khim, J.S., 2019b. Newly identified AhR-active compounds in the sediments of an industrial area using effect-directed analysis. Environ. Sci. Technol. 53, 10043–10052. https://doi.org/10.1021/acs.est.9b02166.
Kim, S., Hong, S., Lee, J., Kim, T., Yoon, S.J., Lee, J., Choi, K., Kwon, B.-O., Giesy, J.P., Khim, J.S., 2020. Long-term trends of persistent toxic substances and potential toxicities in sediments along the west coast of South Korea. Mar. Pollut. Bull. 151, 110821 https://doi.org/10.1016/j.marpolbul.2019.110821.
Kim, Y., Hong, S., Lee, J., Yoon, S.J., An, Y., Kim, M.-S., Jeong, H.-D., Khim, J.S., 2021. Spatial distribution and source identification of traditional and emerging persistent toxic substances in the offshore sediment of South Korea. Sci. Total Environ. 789, 147996 https://doi.org/10.1016/j.scitotenv.2021.147996.
Koganti, A., Weyand, E.H., Rozett, K., Modi, N., Singh, R., Goldstein, L.S., Roy, T.A., Zhang, F.J., Harvey, R.G., 2000. 7Hbenzo[c]fluorene: a major DNA adduct-forming component of coal tar. Carcinogenesis 21 (8), 1601–1609. https://doi.org/10.1093/carcin/21.5.601.
Kucharova, J., Raclavsky, K., Raclavska, H., 2013. The character of refractory organic matter in domestic furnaces. In: 2013 13th International Conference on Environment and Electrical Engineering (EEEIC). IEEE, pp. 239–243, doi: 10.1109/EEEIC-2.2013.6737915.
Larsen, R.K., Baker, J.E., 2003. Source apportionment of Polycyclic Aromatic Hydrocarbons in the urban atmosphere: a comparison of three methods. Environ. Sci. Technol. 37, 1873–1881. https://doi.org/10.1021/es0206184.
LaVoie, E.J., Tulley-Freiler, L., Bedenko, V., Hoffmann, D., 1983. Mutagenicity of substituted phenanthrenes in Salmonella typhimurium. Mutat. Res. Genet. Tox. 116, 91–102. https://doi.org/10.1016/0165-1218(83)90100-3.
Li, M., Ellis, G.S., 2015. Qualitative and Quantitative Analysis of Dibenzofuran, Alkyldibenzofurans, and Benzo[*b*]naphthofurans in Crude Oils and Source Rock Extracts. Energy Fuels 29, 1421–1430. https://doi.org/10.1021/ef502558a.
Li, H.-Y., Gao, P.-P., Ni, H.-G., 2019a. Emission characteristics of parent and halogenated PAHs in simulated municipal solid waste incineration. Sci. Total Environ. 665, 11–17. https://doi.org/10.1016/j.scitotenv.2019.02.002.
Li, R., Hua, P., Zhang, J., Krebs, P., 2019b. A decline in the concentration of PAHs in Elbe River suspended sediments in response to a source change. Sci. Total Environ. 663, 438–446. https://doi.org/10.1016/j.scitotenv.2019.01.355.
Li, P., Xue, R., Wang, Y., Zhang, R., Zhang, G., 2015. Influence of anthropogenic activities on PAHs in sediments in a significant gulf of low-latitude developing regions, the Beibu Gulf, South China Sea: distribution, sources, inventory and probability risk. Mar. Pollut. Bull. 90, 218–226. https://doi.org/10.1016/j.marpolbul.2014.10.048.
Lin, T., Hu, L., Guo, Z., Zhang, G., Yang, Z., 2013. Deposition fluxes and fate of polycyclic aromatic hydrocarbons in the Yangtze River estuarine-inner shelf in the East China Sea. Global Biogeochem. Cycles 27, 77–87. https://doi.org/10.1029/2012GB004317.
Liu, G., Zhang, G., Li, X., Li, J., Peng, X., Qi, S., 2005. Sedimentary record of polycyclic aromatic hydrocarbons in a sediment core from the Pearl River Estuary, South China. Mar. Pollut. Bull. 51, 912–921. https://doi.org/10.1016/j.marpolbul.2005.02.038.
Liu, G., Naja, G.M., Kalla, P., Scheidt, D., Gaiser, E., Cai, Y., 2011. Legacy and fate of mercury and methylmercury in the Florida Everglades. Environ. Sci. Technol. 45, 496–501. https://doi.org/10.1021/es101207f.
Liu, L.-Y., Wang, J.-Z., Wei, G.-L., Guan, Y.-F., Wong, C.S., Zeng, E.Y., 2012. Sediment records of polycyclic aromatic hydrocarbons (PAHs) in the continental shelf of China: implications for evolving anthropogenic impacts. Environ. Sci. Technol. 46, 6497–6504. https://doi.org/10.1021/es300474z.
Lu, Q., Yang, Z., Wu, L., Ruan, X., Yang, W., 2015. The temporal distribution, source and potential toxicity of polycyclic aromatic hydrocarbons in a sediment core from an urban lake in Wuhan, China. Environ. Sci.: Process Impacts 17, 825–834. https://doi.org/10.1039/C4EM00698D.
Luo, W., Wang, T., Jiao, W.T., Hu, W.Y., Naile, J.E., Khim, J.S., Giesy, J.P., Lu, Y., 2012. Mercury in coastal watersheds along the Chinese Northern Bohai and Yellow Seas. J. Hazard. Mater. 215, 199–207. https://doi.org/10.1016/j.jhazmat.2012.02.052.
Ma, X., Han, X., Jiang, Q., Huang, C., Huang, T., Yang, H., Yao, L., 2018. Historical records and source apportionment of polycyclic aromatic hydrocarbons over the past 100 Years in dianchi lake, a plateau lake in southwest China. Arch. Environ. Contam. Toxicol. 75, 187–198. https://doi.org/10.1007/s00244-018-0525-y.
Ma, X., Wan, H., Zhou, J., Luo, D., Huang, T., Yang, H., Huang, C., 2020. Sediment record of polycyclic aromatic hydrocarbons in Dianchi lake, southwest China: influence of energy structure changes and economic development. Chemosphere 248, 126015. https://doi.org/10.1016/j.chemosphere.2020.126015.

McGrath, T., Sharma, R., Hajaligol, M., 2001. An experimental investigation into the formation of polycyclic-aromatic hydrocarbons (PAH) from pyrolysis of biomass materials. Fuel 80, 1787–1797. https://doi.org/10.1016/S0016-2361(01)00062-X.

Meng, J., Hong, S., Wang, T., Li, Q., Yoon, S.J., Lu, Y., Giesy, J.P., Khim, J.S., 2017. Traditional and new POPs in environments along the Bohai and Yellow Seas: an overview of China and South Korea. Chemosphere 169, 503–515. https://doi.org/10.1016/j.chemosphere.2016.11.108.

Mimura, J., Fujii-Kuriyama, Y., 2003. Functional role of AhR in the expression of toxic effects by TCDD. Biochim. Biophys. Acta Gen. Subj. 1619, 263–268. https://doi.org/10.1016/S0304-4165(02)00485-3.

Miyake, Y., Tokumura, M., Wang, Q., Amagai, T., Horii, Y., Kannan, K., 2017. Mechanism of formation of chlorinated pyrene during combustion of polyvinyl chloride. Environ. Sci. Technol. 51, 14100–14106. https://doi.org/10.1021/acs.est.7b04854.

Ministry of Environment of Korea (MOE), 2014. Report on the Effect of the Regulation to Dioxin Emission. Ministry of Environment of Korea, Seoul, Korea (in Korean). https://www.me.go.kr/home/web/board/read.do?boardMasterId=1&boardId=342887&menuId=286.

Myers, A.L., Watson-Leung, T., Jobst, K.J., Shen, L., Besevic, S., Organtini, K., Dorman, F. L., Mabury, S.A., Reiner, E.J., 2014. Complementary nontargeted and targeted mass spectrometry techniques to determine bioaccumulation of halogenated contaminants in freshwater species. Environ. Sci. Technol. 48, 13844–13854. https://doi.org/10.1021/es503090s.

Ohura, T., Morita, M., Makino, M., Amagai, T., Shimoi, K., 2007. Aryl hydrocarbon receptor-mediated effects of chlorinated polycyclic aromatic hydrocarbons. Chem. Res. Toxicol. 20, 1237–1241. https://doi.org/10.1021/tx700148b.

Ohura, T., Sawada, K.-I., Amagai, T., Shinomiya, M., 2009. Discovery of novel halogenated polycyclic aromatic hydrocarbons in urban particulate matters: occurrence, photostability, and AhR activity. Environ. Sci. Technol. 43, 2269–2275. https://doi.org/10.1021/es803633d.

Ohura, T., Morita, M., Kuruto-Niwa, R., Amagai, T., Sakakibara, H., Shimoi, K., 2010. Differential action of chlorinated polycyclic aromatic hydrocarbons on aryl hydrocarbon receptor-mediated signaling in breast cancer cells. Environ. Toxicol. 25, 180–187. https://doi.org/10.1002/tox.20488.

Ohura, T., Sakakibara, H., Watanabe, I., Shim, W.J., Manage, P.M., Guruge, K.S., 2015. Spatial and vertical distributions of sedimentary halogenated polycyclic aromatic hydrocarbons in moderately polluted areas of Asia. Environ. Pollut. 196, 331–340. https://doi.org/10.1016/j.envpol.2014.10.028.

Ohura, T., Horii, Y., Yamashita, N., 2018. Spatial distribution and exposure risks of ambient chlorinated polycyclic aromatic hydrocarbons in Tokyo Bay area and network approach to source impacts. Environ. Pollut. 232, 367–374. https://doi.org/10.1016/j.envpol.2017.09.037.

Onodera, S., Igarashi, K., Fukuda, A., Ouchi, J., Suzuki, S., 1994. Mutagenic potentials of anthracene and phenanthrene compounds during water disinfection with chlorine. Eisei kagaku 40, 233–243. https://doi.org/10.1248/jhs1956.40.233.

Paatero, P., Tapper, U., 1994. Positive matrix factorization: a non-negative factor model with optimal utilization of error estimates of data values. Environmetrics 5 (2), 111–126. https://doi.org/10.1002/env.3170050203.

Pintado-Herrera, M.G., Wang, C., Lu, J., Chang, Y.-P., Chen, W., Li, X., Lara-Martín, P.A., 2017. Distribution, mass inventories, and ecological risk assessment of legacy and emerging contaminants in sediments from the Pearl River Estuary in China. J. Hazard. Mater. 323, 128–138. https://doi.org/10.1016/j.jhazmat.2016.02.046.

Qin, Y., Zheng, B., Lei, K., Lin, T., Hu, L., Guo, Z., 2011. Distribution and mass inventory of polycyclic aromatic hydrocarbons in the sediments of the south Bohai Sea. China. Mar. Pollut. Bull. 62, 371–376. https://doi.org/10.1016/j.marpolbul.2010.09.028.

Ravindra, K., Sokhi, R., Van Grieken, R., 2008. Atmospheric polycyclic aromatic hydrocarbons: source attribution, emission factors and regulation. Atmos. Environ. 42, 2895–2921. https://doi.org/10.1016/j.atmosenv.2007.12.010.

Rogge, W.F., Hildemann, L.M., Mazurek, M.A., Cass, G.R., Simoneit, B.R.T., 1993. Sources of fine organic aerosol 2. noncatalyst and catalyst-equipped automobiles and heavy-duty diesel trucks. Environ. Sci. Technol. 27, 636–651. https://doi.org/10.1021/es00041a007.

Sei, K., Wang, Q., Tokumura, M., Miyake, Y., Amagai, T., 2021. Accurate and ultrasensitive determination of 72 parent and halogenated polycyclic aromatic hydrocarbons in a variety of environmental samples via gas chromatography–triple quadrupole mass spectrometry. Chemosphere 271, 129535. https://doi.org/10.1016/j.chemosphere.2021.129535.

Sun, J.-L., Ni, H.-G., Zeng, H., 2011. Occurrence of chlorinated and brominated polycyclic aromatic hydrocarbons in surface sediments in Shenzhen, South China and its relationship to urbanization. J. Environ. Monit. 13, 2775–2781. https://doi.org/10.1039/C1EM10465A.

Sun, J.-L., Ni, H.-G., Zeng, H., 2012. Ecological risk assessment of parent and halogenated polycyclic aromatic hydrocarbons in surface sediments from an urban river in south China. Environ. Toxicol. Chem. 31, 1867–1873. https://doi.org/10.1002/etc.1890.

Tang, Z., Guo, J.Y., Liao, H.Q., Zhao, X.L., Wu, F.C., Zhu, Y.R., Zhang, L., Giesy, J.P., 2015. Spatial and temporal distribution and sources of polycyclic aromatic hydrocarbons in sediments of Taihu Lake, eastern China. Environ. Sci. Pollut. Res. 22, 5350–5358. https://doi.org/10.1007/s11356-014-3746-2.

Tian, K., Wu, Q., Liu, P., Hu, W., Huang, B., Shi, B., Zhou, Y., Kwon, B.-O., Choi, K., Ryu, J., 2020. Ecological risk assessment of heavy metals in sediments and water from the coastal areas of the Bohai Sea and the Yellow Sea. Environ. Int. 136, 105512 https://doi.org/10.1016/j.envint.2020.105512.

Tolosa, I., Bayona, J.M., Albaigés, J., 1996. Aliphatic and polycyclic aromatic hydrocarbons and sulfur/oxygen derivatives in northwestern Mediterranean sediments: spatial and temporal variability, fluxes, and budgets. Environ. Sci. Technol. 30, 2495–2503. https://doi.org/10.1021/es950647x.

Venkatesan, M., 1988. Occurrence and possible sources of perylene in marine sediments-a review. Mar. Chem. 25, 1–27. https://doi.org/10.1016/0304-4203(88)90011-4.

Vuong, Q.T., Kim, S.-J., Nguyen, T.N.T., Thang, P.Q., Lee, S.-J., Ohura, T., Choi, S.-D., 2020a. Passive air sampling of halogenated polycyclic aromatic hydrocarbons in the largest industrial city in Korea: Spatial distributions and source identification. J. Hazard. Mater. 382, 121238 https://doi.org/10.1016/j.jhazmat.2019.121238.

Vuong, Q.T., Thang, P.Q., Nguyen, T.N.T., Ohura, T., Choi, S.-D., 2020b. Seasonal variation and gas/particle partitioning of atmospheric halogenated polycyclic aromatic hydrocarbons and the effects of meteorological conditions in Ulsan, South Korea. Environ. Pollut. 263, 114592 https://doi.org/10.1016/j.envpol.2020.114592.

Wang, Y., Liu, R.H., Fan, D.J., Yu, P., Wang, J.Y., Tang, A.K., 2013. Distribution and accumulation characteristics of heavy metals in sediments in southern sea area of Huludao City. China. Chin. Geogr. Sci. 23, 194–202. https://doi.org/10.1007/s11769-012-0579-0.

Wang, J., Wu, W., Henkelmann, B., You, L., Kettrup, A., Schramm, K.-W., 2003. Presence of estrogenic activity from emission of fossil fuel combustion as detected by a recombinant yeast bioassay. Atmos. Environ. 37 (23), 3225–3235. https://doi.org/10.1016/S1352-2310(03)00320-0.

Wang, C., Zou, X., Gao, J., Zhao, Y., Yu, W., Li, Y., Song, Q., 2016. Pollution status of polycyclic aromatic hydrocarbons in surface sediments from the Yangtze River Estuary and its adjacent coastal zone. Chemosphere 162, 80–90. https://doi.org/10.1016/j.chemosphere.2016.07.075.

Wang, C., Zou, X., Zhao, Y., Li, Y., Song, Q., Wang, T., Yu, W., 2017. Distribution pattern and mass budget of sedimentary polycyclic aromatic hydrocarbons in shelf areas of the Eastern China Marginal Seas. J. Geophys. Res. Oceans 122, 4990–5004. https://doi.org/10.1002/2017JC012890.

Wang, C., Yu, L., Zou, Y., Ji, L., Li, Y., 2020. Sources and historical sedimentary record: temporal variability of n-alkane and PAHs from the Yellow River Estuary. China. Appl. Geochem. 114, 104475 https://doi.org/10.1016/j.apgeochem.2019.104475.

Wania, F., Mackay, D., 1996. Peer reviewed: tracking the distribution of persistent organic pollutants. Environ. Sci. Technol. 30, 390A–396A. https://doi.org/10.1021/es962399q.

Wei, H., Liu, G.B., Yong, T., Qin, Z., 2015. Emission of polycyclic aromatic hydrocarbons from different types of motor vehicles' exhaust. Environ. Earth Sci. 74, 5557–5564. https://doi.org/10.1007/s12665-015-4570-9.

Yan, W., Chi, J., Wang, Z., Huang, W., Zhang, G., 2009. Spatial and temporal distribution of polycyclic aromatic hydrocarbons (PAHs) in sediments from Daya Bay, South China. Environ. Pollut. 157, 1823–1830. https://doi.org/10.1016/j.envpol.2009.01.023.

Yim, J., Kwon, B.-O., Nam, J., Hwang, J.H., Choi, K., Khim, J.S., 2018. Analysis of forty years long changes in coastal land use and land cover of the Yellow Sea: The gains or losses in ecosystem services. Environ. Pollut. 241, 74–84. https://doi.org/10.1016/j.envpol.2018.05.058.

Yoon, S.J., Hong, S., Kim, S., Lee, J., Kim, T., Kim, B., Kwon, B.-O., Zhou, Y., Shi, B., Liu, P., 2020. Large-scale monitoring and ecological risk assessment of persistent toxic substances in riverine, estuarine, and coastal sediments of the Yellow and Bohai seas. Environ. Int. 137, 105517 https://doi.org/10.1016/j.envint.2020.105517.

Zeng, Q., Jeppesen, E., Gu, X., Mao, Z., Chen, H., 2018. Distribution, fate and risk assessment of PAHs in water and sediments from an aquaculture-and shipping-impacted subtropical lake, China. Chemosphere 201, 612–620. https://doi.org/10.1016/j.chemosphere.2018.03.031.

Zhang, P., Jinming, S., Jie, F., Zhigang, L., Xuegang, L., Huamao, Y., 2009. One century record of contamination by polycyclic aromatic hydrocarbons and polychlorinated biphenyls in core sediments from the southern Yellow Sea. J. Environ. Sci. 21, 1080–1088. https://doi.org/10.1016/S1001-0742(08)62385-2.

Zhang, J., Li, R., Zhang, X., Bai, Y., Cao, P., Hua, P., 2019. Vehicular contribution of PAHs in size dependent road dust: a source apportionment by PCA-MLR, PMF, and Unmix receptor models. Sci. Total Environ. 649, 1314–1322. https://doi.org/10.1016/j.scitotenv.2018.08.410.

Zhang, Y., Tao, S., Cao, J., Coveney, R.M., 2007. Emission of polycyclic aromatic hydrocarbons in China by county. Environ. Sci. Technol. 41, 683–687. https://doi.org/10.1021/es061545h.

Zhang, R., Zhang, F., Zhang, T.-C., 2013. Sedimentary records of PAHs in a sediment core from tidal flat of Haizhou Bay. China. Sci. Total Environ. 450, 280–288. https://doi.org/10.1016/j.scitotenv.2013.02.029.

Zheng, N., Wang, Q., Liang, Z., Zheng, D., 2008. Characterization of heavy metal concentrations in the sediments of three freshwater rivers in Huludao City, Northeast China. Environ. Pollut. 154, 135–142. https://doi.org/10.1016/j.envpol.2008.01.00.

<Supplementary Materials>

Historical trends of traditional, emerging, and halogenated polycyclic aromatic hydrocarbons recorded in core sediments from the coastal areas of the Yellow and Bohai seas

Seo Joon Yoon, Seongjin Hong*, Junghyun Lee, Jongmin Lee, Youngnam Kim, Moo Joon Lee, Jongseong Ryu, Kyungsik Choi, Bong-Oh Kwon, Wenyou Hu, Tieyu Wang, Jong Seong Khim*

This file includes:

Number of pages: 15

Number of Supplementary Tables: 4, Tables S1 to S4

Number of Supplementary Figures: 8, Figs. S1 to S8

References

***Corresponding authors.**

E-mail addresses: hongseongjin@cnu.ac.kr (S. Hong); jskocean@snu.ac.kr (J.S. Khim).

Supplementary Tables

Table S1. Target compounds, abbreviations, target ions in the instrumental analysis, method detection limits, and recovery of surrogate standards.

Target compounds	Abbreviation	Target ions (m/z)		Method detection limit (ng g^{-1} dw)
		Quantification ion	Confirmation ion	
Traditional-Polycyclic aromatic hydrocarbons (t-PAHs)				
Acenaphthylene	Acl	152	151	0.11
Acenaphthene	Ace	153	154	0.19
Fluorene	Flu	166	165	0.21
Phenanthrene	Phe	178	176	0.13
Anthracene	Ant	178	176	0.07
Fluoranthene	Fl	202	200	0.89
Pyrene	Py	202	200	0.05
Benzo[*a*]anthracene	BaA	228	226	0.11
Chrysene	Chr	228	226	0.09
Benzo[*b*]fluoranthene	BbF	252	253	0.09
Benzo[*k*]fluoranthene	BkF	252	253	0.14
Benzo[*a*]pyrene	BaP	252	253	0.13
Indeno[1,2,3-*cd*]pyrene	IcdP	276	138	0.12
Dibenz[*a,h*]anthracene	DbahA	278	276	0.14
Benzo[*g,h,i*]perylene	BghiP	276	138	0.15
Emerging-Polycyclic aromatic hydrocarbons (e-PAHs)				
2-Methylanthracene	2MA	192	191	0.81
9-Ethylphenanthrene	9EP	191	206	0.06
Benzo[*b*]naphtho[2,3-*d*]furan	BBNF	218	189	0.32
11H-Benzo[b]fluorene	11BF	216	215	0.23
Benzo[*b*]naphtho[2,1-*d*]thiophene	BBNT	234	235	0.12
5-Methylbenzo[*a*]anthracene	5MBA	256	241	0.20
1,12-Dimethylbenzo[c]phenanthrene	BCP	242	241	0.34
Benzo[*j*]fluoranthene	BJF	252	253	0.52
Benzo[*e*]pyrene	BEP	252	250	0.28
Halogenated-Polycyclic aromatic hydrocarbons (Hl-PAHs)				
9-Bromofluorene	9-Br-Flu	165	166	1.07
2-Bromofluorene	2-Br-Flu	165	176	0.58
9-Chlorophenanthrene	9-Cl-Phe	212	176	0.53
2-Chloroanthracene	2-Cl-Ant	212	176	1.21
9-Chloroanthracene	9-Cl-Ant	212	214	0.61
3-Bromophenanthrene	3-Br-Phe	256	176	0.57
9-Bromophenanthrene	9-Br-Phe	256	176	1.01
2-Bromophenanthrene	2-Br-Phe	256	176	0.78
1-Bromoanthracene	1-Br-Ant	256	258	0.51
2-Bromoanthracene	2-Br-Ant	258	256	0.90
9-Bromoanthracene	9-Br-Ant	256	176	0.87
9,10-Dichlorophenanthrene	9,10-Cl-Phe	246	248	0.25
9,10-Dichloroanthracene	9,10-Cl-Ant	246	176	0.57
2,7-Dibromofluorene	2,7-Br-Flu	163	245	0.79
3-Chlorofluoranthene	3-Cl-Fluo	236	200	0.75
1-Chloropyrene	1-Cl-Py	236	200	0.46
3-Bromofluoranthene	3-Br-Fluo	282	280	0.62
1,8-Dibromoanthracene	1,8-Br-Ant	176	336	0.63
9,10-Dibromoanthracene	9,10-Br-Ant	176	336	0.67
2,7-Dibromophenanthrene	2,7-Br-Phe	176	336	0.70
1-Bromopyrene	1-Br-Py	280	282	0.63
1,8-Dichloropyrene	1,8-Cl-Py	270	200	0.53
1,3,6-Trichloropyrene	1,3,6-Cl-Py	304	306	0.54
1,6-Dibromopyrene	1,6-Br-Py	360	200	1.19
1,8-Dibromopyrene	1,8-Br-Py	200	360	1.27

Table S1. (continued).

Target compounds	Abbreviation	Target ions (*m/z*)		Method detection limit (ng g^{-1} dw)
		Quantification ion	Confirmation ion	
Halogenated-Polycyclic aromatic hydrocarbons (Hl-PAHs)				
7-Bromobenz[*a*]anthracene	7-Br-BaA	226	306	0.41
4-Bromobenz[*a*]anthracene	4-Br-BaA	306	226	0.79
1,3,6,8-Tetrachloropyrene	1,3,6,8-Cl-Py	340	338	0.39
6,12-Dibromochrysene	6,12-Br-Chr	226	286	0.83
6-Bromobenzo[*a*]pyrene	6-Br-BaP	330	332	0.32
Target compounds		**Quantification ion**	**Confirmation ion**	**%Recovery (Mean ± SD)**
Surrogate standards				
Acenaphthene-d_{10}		164	162	78 ± 18
Phenanthrene-d_{10}		188	189	83 ± 9
Chrysene-d_{12}		240	236	94 ± 10
Perylene-d_{12}		264	270	86 ± 12

Table S2. Instrumental conditions of the gas chromatograph equipped with a mass selective detector for analyzing traditional, emerging, and halogenated PAHs.

GC/MSD system	**Agilent 7890B GC and 5977B MSD**
Column	DB-5MS UI (30 m long, 0.25 mm i.d., 0.25 μm film thickness)
Gas flow	1 mL/min He
Injection mode	Splitless
Injection volume	2 μL
Injector temperature	300 °C
Ionization	EI mode (70 eV)
MS temperature	180 °C
Detector temperature	230 °C
Oven temperature	60 °C hold 2 min
(t-PAHs, e-PAHs)	Increase 6 °C/min to 300 °C
	300 °C hold 13 min
Oven temperature	60 °C hold 2 min
(Hl-PAHs)	Increase 15 °C/min to 200 °C hold 20min
	Increase 4 °C/min to 300 °C hold 2min

Table S3. Relative potency-normalized BaP activity (REP_{BaP}), mean toxicity equivalency concentrations (TEQs), and contributions of target PAHs.

Compounds	REP_{BaP}[a]	pg-TEQ g^{-1}	Contribution (%)
t-PAHs			
Phe	0.004	0.51	0.158
Ant	0.01	0.12	0.072
Fl	0.01	1.0	0.62
Py	0.05	4.4	2.6
BaA	1.4	60.9	36.1
Chr	2.5	75.9	45.0
BaP	1.0	29.6	15.4
ΣPAHs		172	99.96
e-PAHs			
BEP	0.005	0.038	0.019
Cl-PAHs			
9,10-Cl-Phe	0.16	0.013	0.005
Br-PAHs			
2-Br-Flu	0.02	0.018	0.0013
1-Br-Py	0.04	0.029	0.0007
7-Br-BaA	0.84	0.410	0.01
6-Br-BaP	0.002	0.003	0.0006
ΣBr-PAHs		0.459	0.0127

[a] Relative potency of t-PAHs, e-PAHs, Cl-PAHs, and Br-PAHs refed Ohura et al. (2007, 2009, 2018).

Table S4. Diagonostic ratios of specific Hl-PAHs from the industrial sources of this study and previous studies.

Source	Matrix	1-Cl-Py/3-Cl-Fl	3-Cl-Fl/1-Cl-Py	7-Br-BaA/3-Br-Fl
Waste incinerators [a]	Stack gas	11.8	0.08	-
	Fly ash	1.5	0.65	-
Road Tunnel [b]	Air	2.16–3.80	0.26– 0.46	0.09–6.31
Secondary copper smelting [c]	Stack gas	0.06–4.50	0.22–17.60	0.01–1.79
	Fly ash	0.10–1.35	0.74–10.20	0.04–0.77
Cement kiln co-processing solid waste [d]	Fly ash	0.08–3.01	0.33–11.90	0.03–6.87
This study (HL4)	Sediment	1.10–2.96	0.34– 0.91	0.14

[a] Horii et al. (2008).
[b] Nilsson and Oestman (1993).
[c] Jin et al. (2017).
[d] Jin et al. (2018).

Supplementary Figures

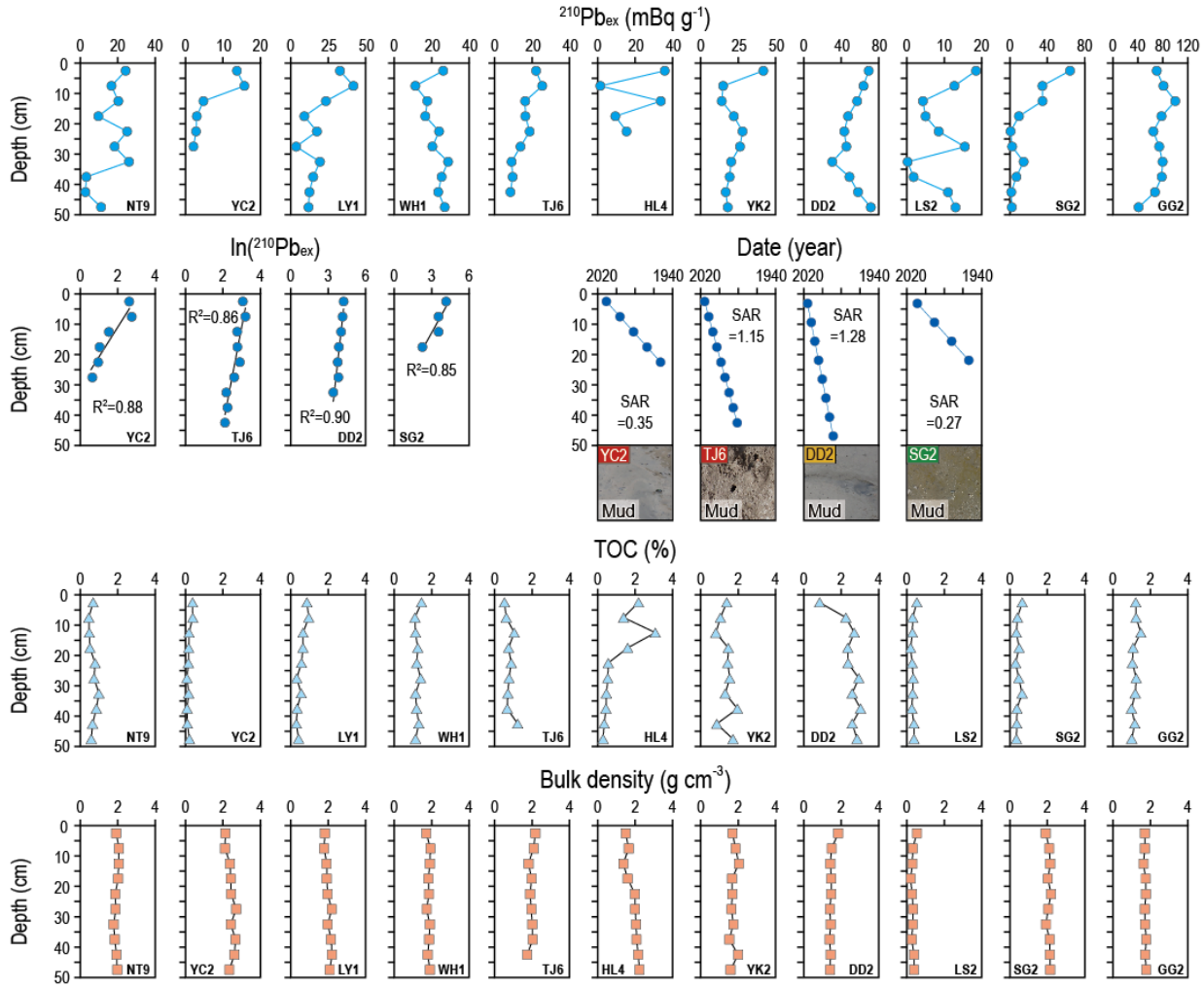

Fig. S1. Depth profiles of unsupported ^{210}Pb ($^{210}Pb_{ex}$), sedimentation rate (SAR), age of sediment, total organic carbon, and bulk density in intertidal sediment cores of the Yellow and Bohai seas. Photographs of each site show the grain size of the sediment.

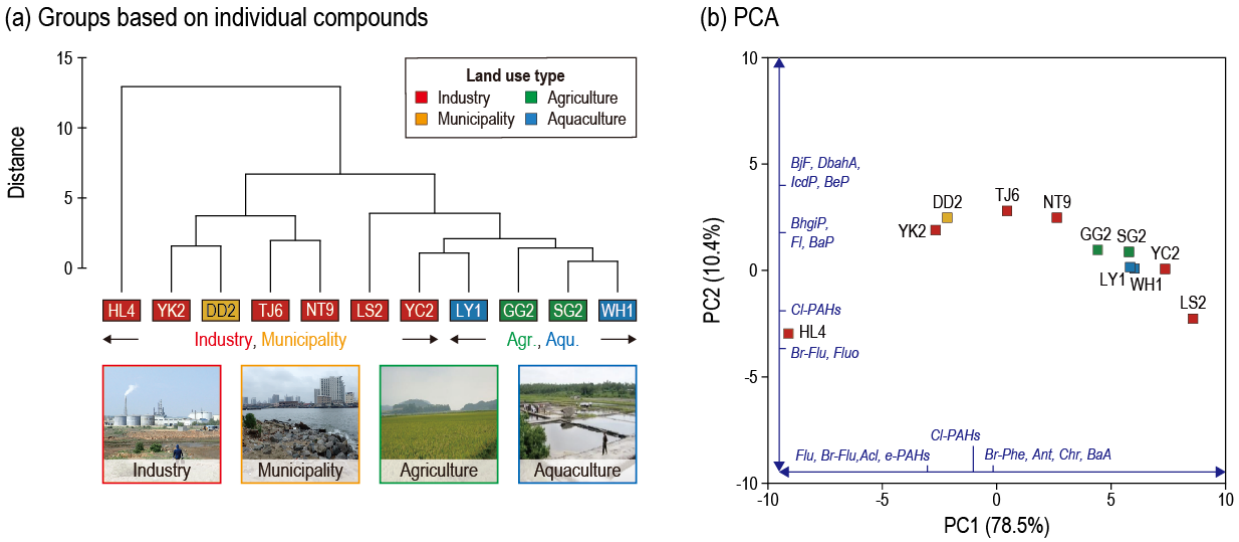

Fig. S2. Results of **(a)** cluster analysis and **(b)** principal component analysis showing the groups based on individual compounds.

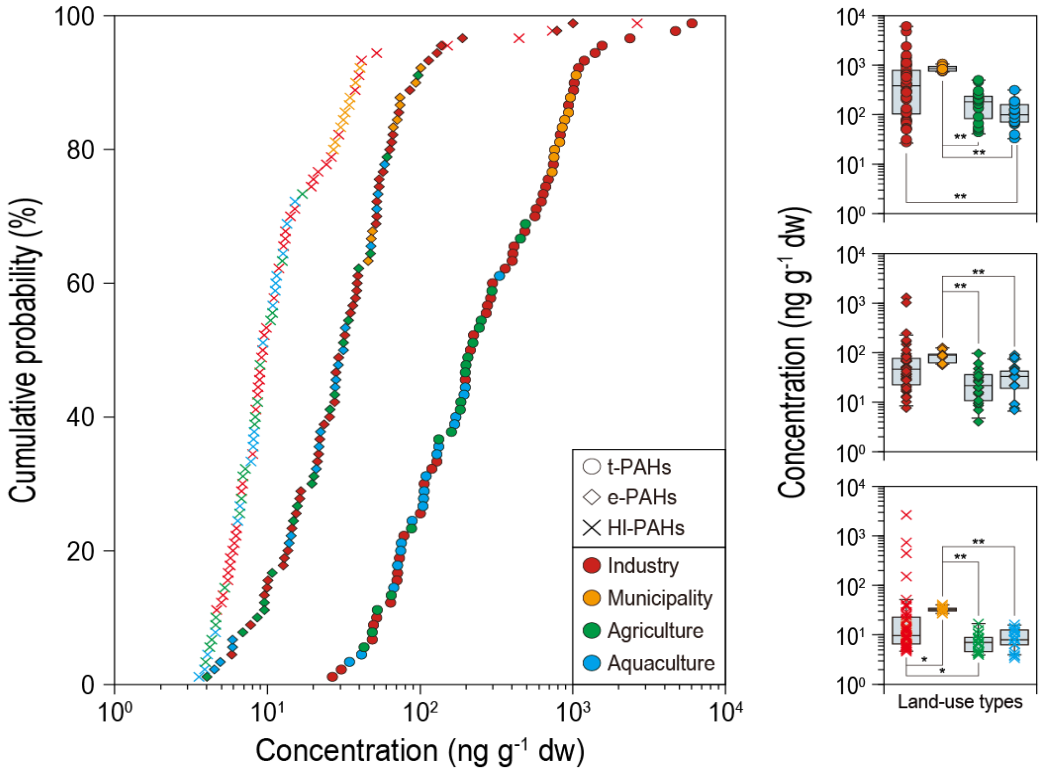

Fig. S3. Cumulative probability and box plot of traditional, emerging, and halogenated PAHs relative to land-use types.

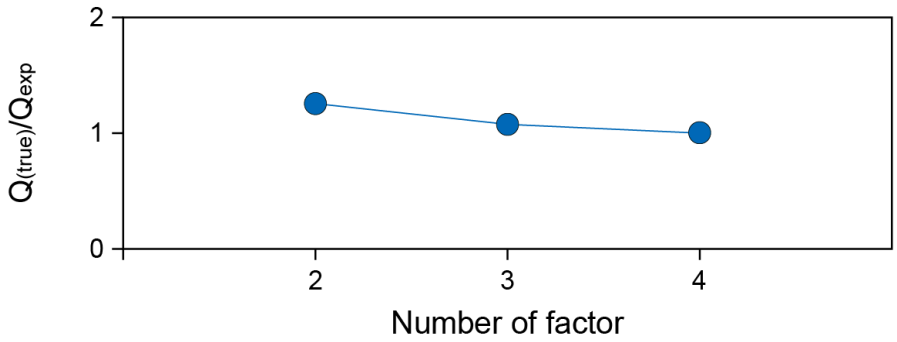

Fig. S4. Q_{True}/Q_{Exp} values of the number of factors derived with a PMF receptor model.

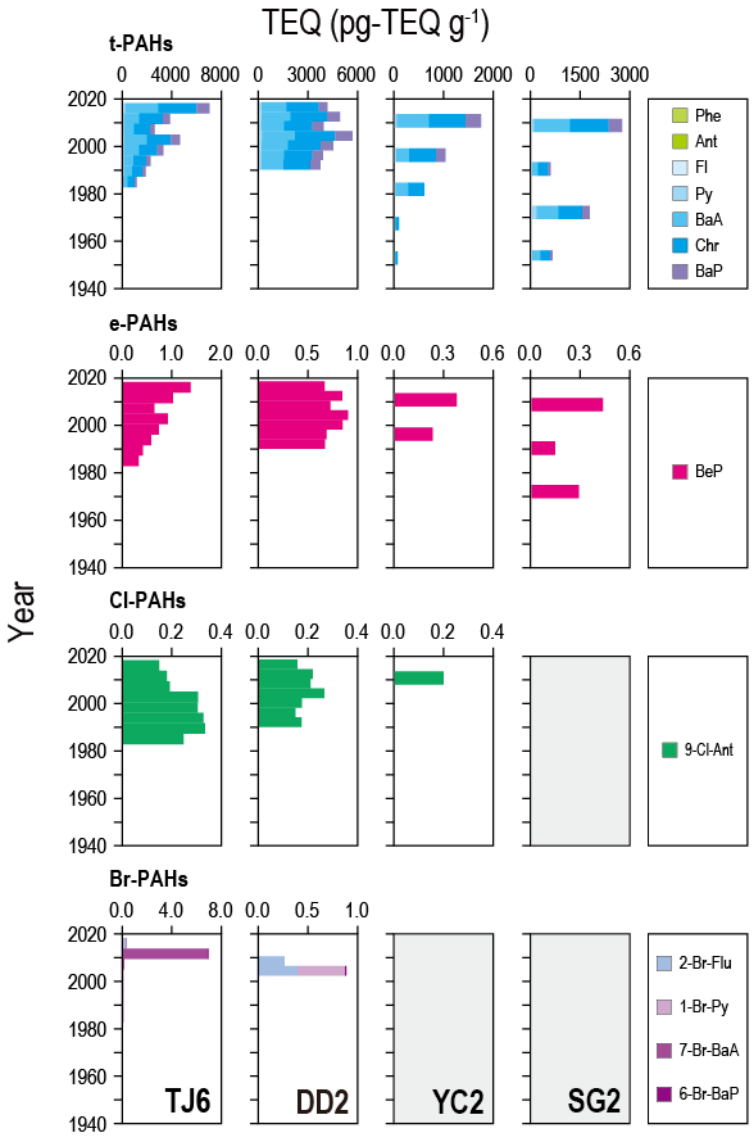

Fig. S5. Historical distribution of toxicity equivalency quantities (TEQs) and contribution of t-PAHs, e-PAHs, Cl-PAHs, and Br-PAHs in each site. The sites for no TEQ values are presented with a gray background.

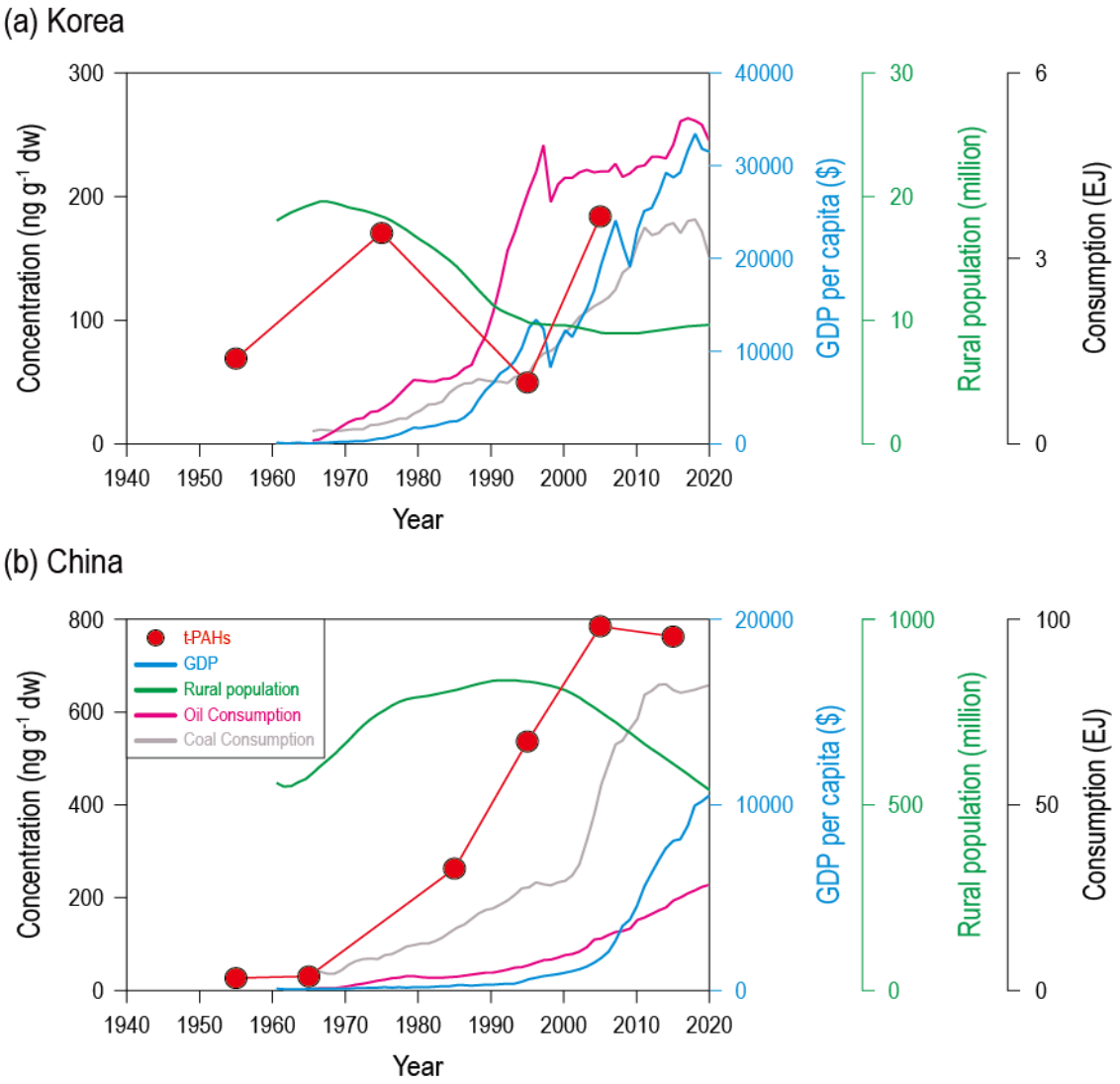

Fig. S6. Historical changes to the concentration of t-PAHs, GDP, rural population, oil consumption, and coal consumption in (a) Korea and (b) China (Looney, 2020).

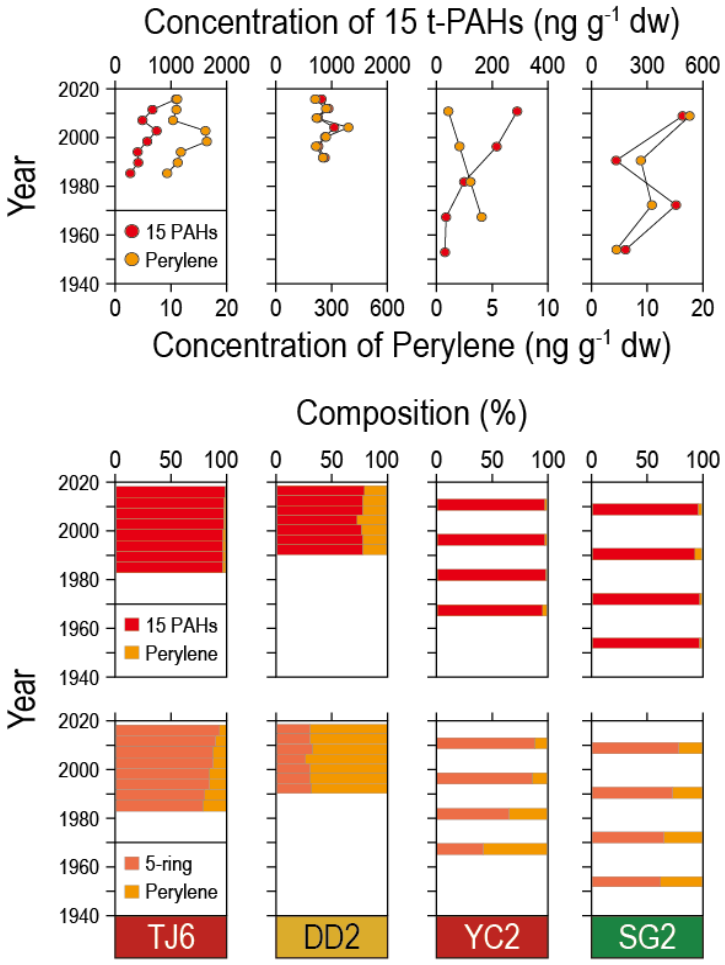

Fig. S7. Historical deposition and relative composition of t-PAHs and perylene. 5-ring t-PAHs include BbF, BkF, and BaP.

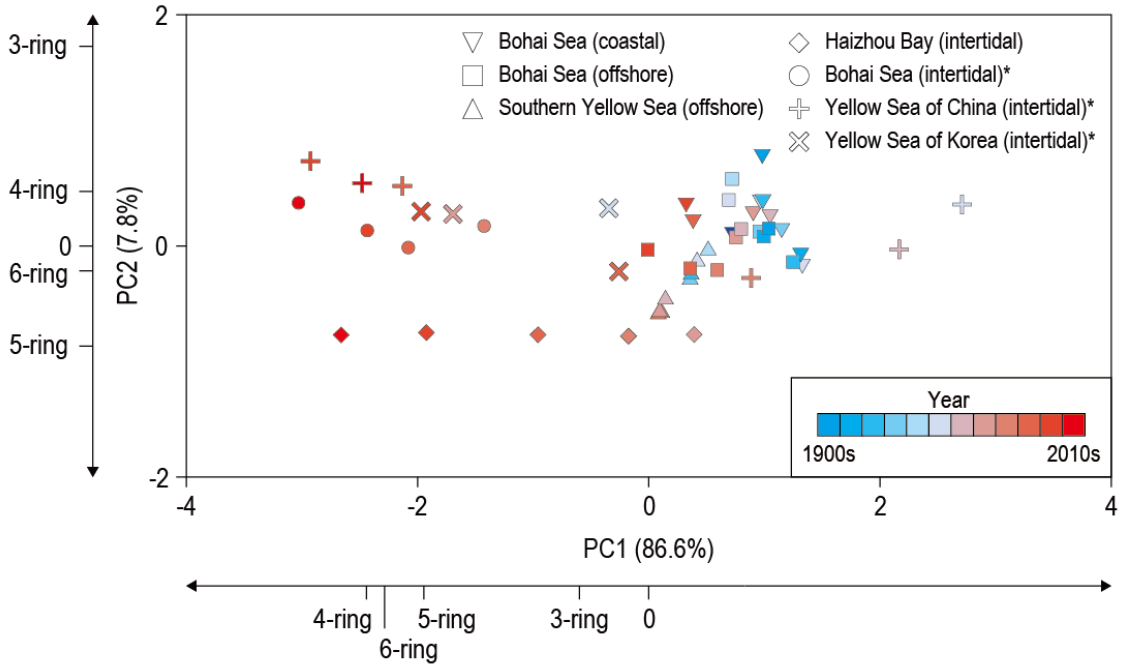

Fig. S8. Principal component analysis using the compositions of 15 t-PAHs in sediments obtained from the present study and previous studies (Zhang et al., 2009; Hu et al., 2011; Zhang et al., 2013; Cai et al., 2016).

References

Cai, Y., Wang, X., Wu, Y., Li, Y., Ya, M., 2016. Over 100-year sedimentary record of polycyclic aromatic hydrocarbons (PAHs) and organochlorine compounds (OCs) in the continental shelf of the East China Sea. Environ. Pollut. 219, 774–784.

Horii, Y., Ok, G., Ohura, T., Kannan, K., 2008. Occurrence and profiles of chlorinated and brominated polycyclic aromatic hydrocarbons in waste incinerators. Environ. Sci. Technol. 42, 1904–1909.

Hu, L., Guo, Z., Shi, X., Qin, Y., Lei, K., Zhang, G., 2011. Temporal trends of aliphatic and polyaromatic hydrocarbons in the Bohai Sea, China: evidence from the sedimentary record. Org. Geochem. 42, 1181–1193.

Jin, R., Yang, L. , Zheng, M. , Xu, Y. , Li, C. , Liu, G., 2018. Source identification and quantification of chlorinated and brominated polycyclic aromatic hydrocarbons from cement kilns co-processing solid wastes. Environ. Pollut. 242, 1346–1352.

Jin, R., Liu, G., Zheng, M., Jiang, X., Zhao, Y., Yang, L., Wu. X., Xu, Y., 2017. Secondary copper smelters as sources of chlorinated and brominated polycyclic aromatic hydrocarbons. Environ. Sci. Technol. 51, 7945–7953.

Looney, B., 2020. Statistical Review of World Energy, 2020. Bp. Statistical Review, London, UK, accessed 2020.

Nilsson, U.L., Oestman, C.E., 1993. Chlorinated polycyclic aromatic hydrocarbons: method of analysis and their occurrence in urban air. Environ. Sci. Technol. 27, 1826–1831.

Ohura, T., Morita, M., Makino, M., Amagai, T., Shimoi, K., 2007. Aryl hydrocarbon receptor-mediated effects of chlorinated polycyclic aromatic hydrocarbons. Chem. Res. Toxicol. 20, 1237–1241.

Ohura, T., Sawada, K.-i., Amagai, T., Shinomiya, M., 2009. Discovery of novel halogenated polycyclic aromatic hydrocarbons in urban particulate matters: occurrence, photostability, and AhR activity. Environ. Sci. Technol. 43, 2269-2275.

Ohura, T., Horii, Y., Yamashita, N., 2018. Spatial distribution and exposure risks of ambient chlorinated polycyclic aromatic hydrocarbons in Tokyo Bay area and network approach to source impacts. Environ. Pollut. 232, 367–374.

Zhang, P., Jinming, S., Jie, F., Zhigang, L., Xuegang, L., Huamao, Y., 2009. One century record of contamination by polycyclic aromatic hydrocarbons and polychlorinated biphenyls in core sediments from the southern Yellow Sea. J. Environ. Sci. 21, 1080–1088.

Zhang, R., Zhang, F., Zhang, T.-C., 2013. Sedimentary records of PAHs in a sediment core from tidal flat of Haizhou Bay, China. Sci. Total Environ. 450, 280–288.